



HAL
open science

Direct contact, dissolution and generation of reactive oxygen species: How to optimize the antibacterial effects of layered double hydroxides

Jazia Awassa, Damien Cornu, Christian Ruby, Sofiane El-Kirat-Chatel

► To cite this version:

Jazia Awassa, Damien Cornu, Christian Ruby, Sofiane El-Kirat-Chatel. Direct contact, dissolution and generation of reactive oxygen species: How to optimize the antibacterial effects of layered double hydroxides. *Colloids and Surfaces B: Biointerfaces*, 2022, 217, pp.112623. 10.1016/j.colsurfb.2022.112623 . hal-03707352

HAL Id: hal-03707352

<https://hal.science/hal-03707352>

Submitted on 28 Jun 2022

HAL is a multi-disciplinary open access archive for the deposit and dissemination of scientific research documents, whether they are published or not. The documents may come from teaching and research institutions in France or abroad, or from public or private research centers.

L'archive ouverte pluridisciplinaire **HAL**, est destinée au dépôt et à la diffusion de documents scientifiques de niveau recherche, publiés ou non, émanant des établissements d'enseignement et de recherche français ou étrangers, des laboratoires publics ou privés.



Distributed under a Creative Commons Attribution - NonCommercial - NoDerivatives 4.0 International License

1 **Direct contact, dissolution and generation of reactive oxygen species:**

2 **How to optimize the antibacterial effects of layered double hydroxides**

3 Jazia Awassa, Damien Cornu*, Christian Ruby, Sofiane El-Kirat-Chatel

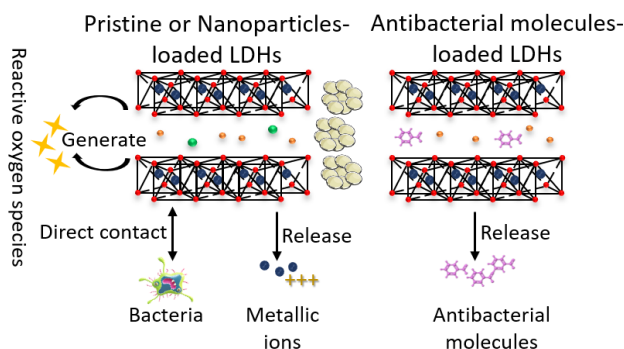
4 *Université de Lorraine, CNRS, LCPME, F-54000 Nancy, France*

5 *Corresponding author:

6 Damien Cornu: Damien.cornu@univ-lorraine.fr

7 **Abstract**

8 Infections by pathogenic bacteria have been threatening several fields as food industries,
9 agriculture, textile industries and healthcare products. Layered double hydroxides materials
10 (LDHs), also called anionic clays, could be utilized as efficient antibacterial materials due to their
11 several interesting properties such as ease of synthesis, tunable chemical composition,
12 biocompatibility and anion exchange capacity. Pristine LDHs as well as LDH-composites
13 including antibacterial molecules and nanoparticles loaded-LDHs were proven to serve as efficient
14 antibacterial agents against various Gram-positive and Gram-negative bacterial strains. The
15 achieved antibacterial effect was explained by the following mechanisms: (1) Direct contact
16 between the materials and bacterial cells driven by electrostatic interactions between positively
17 charged layers and negatively charged cell membranes, (2) Dissolution and gradual release over
18 time of metallic ions or antibacterial molecules, (3) Generation of reactive oxygen species.



19

20 **Keywords**

21 LDH

22 Antibacterial mechanism

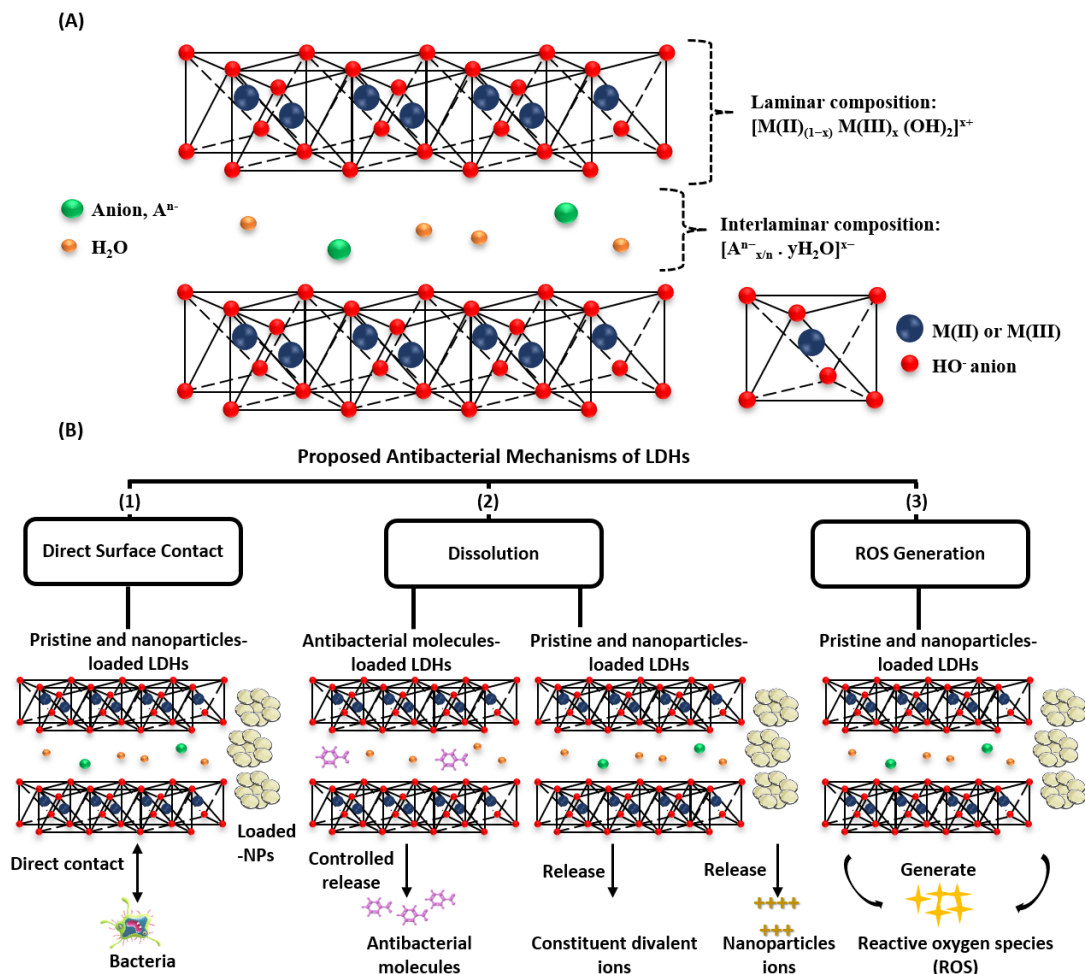
23 Direct contact

- 24 Metallic ions release
- 25 Antibacterial molecules release
- 26 ROS generation

27 1. Introduction

28 Infectious diseases caused by microbial contamination are threatening human health all over the
29 world [1]. Infections by pathogenic microorganisms are of serious concern to several fields such
30 as food industries [2], textile industries [3], healthcare [4], and pharmaceutical products [5].
31 Traditional antibiotic drugs can usually treat bacterial infections, however, their extensive use had
32 led to bacterial resistance and the spread of resistant strains [6,7]. Recent advances in the field of
33 material science had opened up new gates for designing new antimicrobials based on synthetic
34 inorganic materials [8–10] In fact, inorganic antibacterial materials are considered advantageous
35 over organic antibacterial materials due to their higher stability, recyclability and improved safety
36 [11].

37 Among the various inorganic materials, layered double hydroxides (LDHs) were extensively
38 studied due to their interesting properties as anion exchangeability, compositional flexibility, and
39 biocompatibility, thus making them good candidates for several potential applications as catalysis
40 [12,13], sorption of pollutants [14,15], biosensors [16], drug storage delivery [17,18], and
41 antimicrobial materials [12,19–22]. Layered double hydroxides (LDHs), also known as anionic
42 clays, are lamellar solids having a general formula expressed as $[M(II)_{(1-x)}M(III)_x(OH)_2]^{x+} [A^{n-}_{x/n}$
43 $\cdot yH_2O]^{x-}$, where M(II) and M(III) represent divalent and trivalent metallic cations respectively,
44 and A^{n-} is an exchangeable intercalating anion. The LDH structure (**Fig. 1A**) is based on the
45 stacking of positively charged brucite-like sheets comprising the divalent and trivalent cations
46 linked by OH units coordinated at the octahedral positions forming sheets, which are then stacked
47 up on top of each other to yield a layered structure similar to that of brucite mineral $[Mg(OH)_2]$
48 [23–27]. These brucite-like sheets hold a net positive charge which is compensated by negatively
49 charged anions along with water molecules in the interlaminar regions.



50

51 **Fig. 1.** (A) A schematic representation of LDH structure. The lamina composition is made up of positively
 52 charged brucite-like sheets presenting divalent and trivalent metal cations (M(II) and M(III)) octahedrally
 53 linked to hydroxyl groups (HO^-), whereas compensating intercalating anions (A^{n-}) and water molecules are
 54 present in the interlamina region [28]. (B) Proposed antibacterial mechanisms of LDHs. (1): Direct surface
 55 contact interactions between pristine and nanoparticles-loaded LDHs with bacteria, (2) Dissolution of
 56 antibacterial molecules: release of antibacterial molecules by antibacterial molecules-loaded LDHs and
 57 release of metallic ions by pristine and nanoparticles-loaded LDHs (3) Generation of reactive oxygen
 58 species (ROS) by pristine and nanoparticles-loaded LDHs.

59 LDH-based materials were utilized for several biological applications especially antimicrobial
60 ones [8,29,30]. In fact, several surveys showed that LDHs possess high potential as carriers of
61 functional antibacterial molecules as antibiotics because of their high biocompatibility, high
62 chemical stability, and controlled release rate [31–33]. In addition, LDH can also be loaded with
63 nanoparticles (NPs) such as gold, silver, copper and zinc oxide NPs which are known to treat
64 several diseases caused by bacterial infections [19,34–38]. The assembly of metallic NPs-in
65 inorganic matrices as of LDHs can provide an inexpensive and biocompatible means to help limit
66 the problem of aggregation and high exposure dose of free NPs [39]. Moreover, recent studies
67 showed that even pristine LDHs, more precisely Zn and Cu-based pristine LDHs, could induce an
68 efficient antibacterial without any further modification [22,40–43].

69 Each type of antibacterial LDH, *e.g.* antibacterial molecules-loaded LDHs, NPs-loaded LDHs and
70 pristine LDHs, may induce a different antibacterial mode of action. **Fig. 1B** illustrates the three
71 different suggested mechanisms explaining the antimicrobial activity of these different types of
72 antibacterial LDHs: (1) direct surface interactions between pristine and NPs-loaded LDHs with
73 the bacteria thus leading to their growth inhibition or death [39,40,42,44,45], (2) dissolution by
74 through the controlled release of antibacterial molecules present in the LDH interlaminar region
75 of antibacterial molecules-loaded LDH composites [46,47], or through the release of release
76 constituent metallic ions, *e.g.* Zn^{2+} , Cu^{2+} , Ag^{+} from NPs-loaded and pristine LDHs [12,40,43,48],
77 (3) generation of reactive oxygen species (ROS) by pristine and NPs-loaded LDHs to yield an
78 efficient antibacterial effect [16,38,40–42,49]. **Table 1** reports the antibacterial performance of
79 pristine and NPs-loaded LDHs together with the suggested antibacterial mechanisms provided in
80 previous literature.

81 In fact, numerous reviews reported the synthesis routes of LDH materials and their various
82 applications [50–53], however, only a few focused on their antimicrobial effects [8,54–56].
83 Although these reviews explained the efficiency of LDHs to serve as antimicrobial materials, the
84 information given concerned more generally different types of biological applications and not
85 specifically the antimicrobial ones. Moreover, none of these reviews reported in detail the different
86 antibacterial mechanisms occurring at the biointerface between LDHs and bacteria.

87 In this review, several suggested antibacterial mechanisms of the different types of antibacterial
88 LDHs are discussed in three sections. Of course, it is not possible to isolate only one antibacterial
89 mechanism, because some antimicrobial effects of LDHs result from the combination of direct
90 contact, ion or antimicrobial molecules release and ROS generation. However, some specificities
91 can be correlated to the different suggested mechanisms. For instance, the long-distance effect
92 through molecules or ion release, or the effect of light for the ROS generation. Therefore, each
93 section starts with different physico-chemical considerations, followed by various experimental
94 observations of these mechanisms and is concluded with some considerations on how to tune the
95 properties of LDHs to maximize the antimicrobial effect through the suggested mechanism.

96 **Table 1.** Antibacterial performance of pristine and NPs-loaded LDHs and the proposed associated
97 antibacterial mechanisms. MIC values correspond to the minimum inhibitory concentration required to
98 inhibit the growth of a certain bacteria, whereas inhibition zone diameters correspond to the obtained
99 inhibitory diameter zone generated by LDHs when being tested in agar disk or agar well diffusion tests.

LDH sample	Type	Tested Bacteria	Antibacterial performance	Proposed mechanism	Reference
------------	------	-----------------	---------------------------	--------------------	-----------

Ag-ZnAl	NP-loaded LDHs	Gram-positive: <i>Staphylococcus aureus</i> Gram-negative: <i>Escherichia coli</i>	Ag-LDH composite showed a more stable antibacterial activity than unsupported nanosized silver with inhibition zone diameters and MIC values ranging between 7 and 14.7 mm and 0.3 and 0.7 µg/mL, respectively over several days	Surface interactions	[39]
Ag-ZnAl	NP-loaded LDHs	Gram-positive: <i>S. aureus</i> Gram-negative: <i>E. coli</i>	Ag-LDHs showed efficient antibacterial activity with inhibition zone diameters ranging from 8 to 18 mm. Aged samples showed an enhanced antibacterial activity in comparison to samples obtained directly by coprecipitation due to their smaller size enabling more contact with the tested bacteria	Surface interactions	[44]
Ag-MgAl	NP-loaded LDHs	Gram-positive: <i>S. aureus</i> Gram-negative: <i>E. coli</i>	Ag-LDH showed similar antimicrobial activity to that of free Ag NPs with MIC values of 6.6 and 12 µg/mL against <i>S. aureus</i> and <i>E. coli</i> , respectively	Surface interactions	[57]
ZnO-Water polyurethane (WPU)-ZnAl	NP-loaded LDHs	Gram-positive: <i>S. aureus</i> Gram-negative: <i>E. coli</i>	ZnO-WPU-LDH completely inhibited (100% inhibition) the growth of tested bacteria which was validated by plate colony count method	Ions release, generation of ROS	[49]
ZnFe	Pristine LDHs	Gram-positive: <i>S. aureus</i> , <i>Staphylococcus epidermidis</i> , <i>Streptococcus pyogenes</i> Gram-negative: <i>E. coli</i> , <i>Proteus vulgaris</i> , <i>Klebsiella pneumoniae</i> , <i>Pseudomonas aeruginosa</i>	ZnFe LDHs showed an efficient antimicrobial activity very similar to that of conventional antibiotics with inhibition zone diameters of 16.8-22.9 mm depending on the type of tested bacteria and selectivity of LDHs toward different bacterial strains	Surface interactions, metal ions release	[22]
ZnAl	Pristine LDHs	Gram-positive: <i>S. aureus</i> , <i>S. epidermidis</i> Gram-negative: <i>P. aeruginosa</i>	ZnAl LDH samples exhibited an efficient antibacterial activity with MIC values ranging from 4000 to 10000 µg/mL depending on the Zn ^{II} :Al ^{III} molar ratio initially present in the LDH structure	Ions release, generation of ROS	[58]
Ternary CuZnAl	Pristine LDHs	Gram-positive: <i>S. aureus</i> Gram-negative: <i>E. coli</i>	Ternary LDH samples showed increasing antibacterial activities with inhibition zone diameters of 8-15 mm	Surface interactions, ions release	[59]

			depending on the size of LDH particles		
AgCl-ZnAl	NP-loaded LDHs	Gram-negative: <i>E. coli</i>	AgCl-LDHs showed efficient antibacterial activity with MIC values ranging from 3.83 and 9.45 µg/mL depending on the size of the powders	Surface interactions, generations of ROS	[60]
Ag-MgAl	NP-loaded LDHs	Gram-negative: <i>E. coli</i>	Ag-LDHs showed an efficient antibacterial activity with MIC values between 63 and 500 µg/mL depending on the size and amount of loaded Ag NPs.	Ions release, surface interactions	[61]
Au-MgAl	NP-loaded LDHs	Gram-positive: <i>S. aureus</i> Gram-negative: <i>E. coli</i>	Au-LDH inhibited the growth of tested bacteria by 25-100% only when being irradiated with Near Infrared (NIR) laser. Greater bacterial inhibition percentages were achieved with longer irradiation times and greater hybrid loadings	Surface interactions, generations of ROS	[38]
ZnAl	Pristine LDHs	Gram-positive: <i>S. aureus</i> , <i>Streptococcus lactis</i> , <i>Bacillus cereus</i> Gram-negative: <i>E. coli</i> , <i>P. aeruginosa</i> , <i>Salmonella typhimurium</i>	ZnAl LDHs showed an efficient antibacterial activity with inhibition zone diameters of 9-21 mm and MIC values of 150-300 µg/mL depending on the type of tested	Ions release, surface interactions, generation of ROS	[40]
CuAl, NiAl, CoAl, MnAl, MgAl,	Pristine LDHs	Gram-positive: <i>S. aureus</i> Gram-negative: <i>E. coli</i>	LDH samples showed an efficient antibacterial activity with MIC values between 800 and 1500 µg/mL depending on the type of tested LDH sample	Ions release, surface interactions, generation of ROS	[41]
Ternary CuMgAl:CO ₃	Pristine LDHs	Gram-positive: <i>S. aureus</i> , <i>Bacillus subtilis</i> , <i>Enterococcus faecalis</i> Gram-negative: <i>E. coli</i> , <i>P. aeruginosa</i>	Ternary LDH samples showed increasing antibacterial activity with increasing Cu ^{II} :Al ^{III} molar ratio and MIC values up to 31000 µg/mL	Surface interactions, ions release	[42]
ZnAl, CuAl, NiAl, CoAl, MgAl	Pristine LDH	Gram-positive: <i>S. aureus</i> Gram-negative: <i>E. coli</i>	Only ZnAl and CuAl LDHs exhibited an efficient antibacterial effect with inhibition zone diameters ranging from 7 to 13 mm and MIC values of 375 to 12000 µg/mL depending on the concentration of released divalent metallic cations	Ions release	[43]

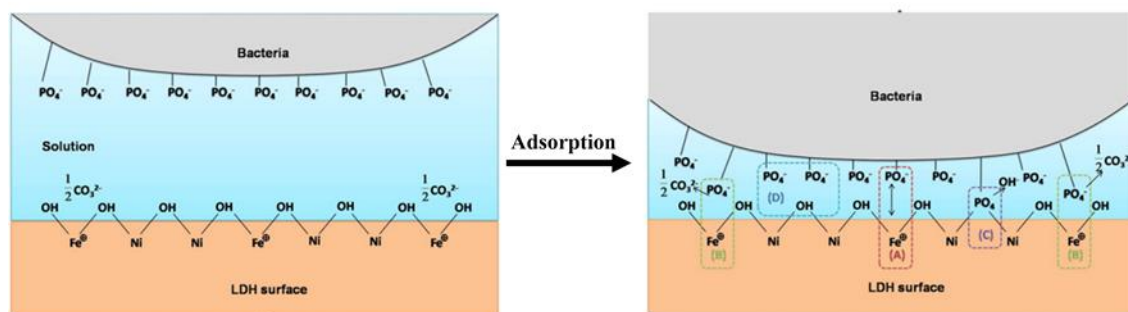
101 2. LDH antibacterial activity by direct surface interactions

102 2.1. Electrostatic interactions between bacteria and LDHs

103 From a physicochemical point of view, microorganisms as bacteria can be considered as living
104 colloidal particles. This is due to their compositional polypeptides having ionizable weakly acidic
105 and basic groups, *e.g.* carboxyl and amino groups [62,63]. Therefore, materials possessing
106 positively charged surfaces are believed to be ideal nuclei for microbial adhesion [64]. LDHs have
107 a positively charged surface with zeta potential values up to 30-50 mV [65], large surface areas of
108 10-200 m²/g [66], and a high anion exchange capacity of 2-5 mmol/g [67], thus meeting all the
109 criteria for an ideal bacterial adhesion.

110 Jin *et al.* reported the removal of Gram-negative bacteria *Escherichia coli* by chloride-intercalated
111 pristine MgAl and ZnAl LDHs for water purification applications [68]. LDH slurry systems
112 showed a bacterial adsorption efficiency $\geq 99\%$. Similarly, the flow-through column showed an
113 adsorption efficiency as high as 87 to 99%. Such findings suggested that LDHs could potentially
114 be used as a sorbent material to purify untreated water from bacteria. Liu *et al.* developed a
115 carbonate intercalated NiFe LDH which was able to adsorb 45-55 mg/g of *Bacillus subtilis* under
116 different experimental conditions [66]. The authors proposed different possible mechanisms of
117 bacteria adsorption onto LDH particle surface including four types of interactions which are
118 sketched in **Fig. 2**. The first suggested interaction involved electrostatic interactions between the
119 negatively charged bacterial membrane (due to the presence of PO₄⁻ groups) and the positively
120 charged LDH surface (**Region A, Fig. 2**). Bacterial adsorption could also be enhanced by anion
121 exchange reactions, where PO₄⁻ groups present at the surface of the bacterium could gradually
122 replace individual CO₃²⁻ on the LDH surface (**Region B, Fig. 2**). Bacterial adsorption could be
123 further achieved by the substitution of the OH groups on the LDH surface with the PO₄⁻ groups

124 (Region C, Fig. 2). The last suggested adhesion mechanism was that PO_4^- groups present on the
 125 bacterial surface and the OH groups on the LDH surface would interact with each other via
 126 hydrogen bonds and/or polar attractions (Region D, Fig. 2).



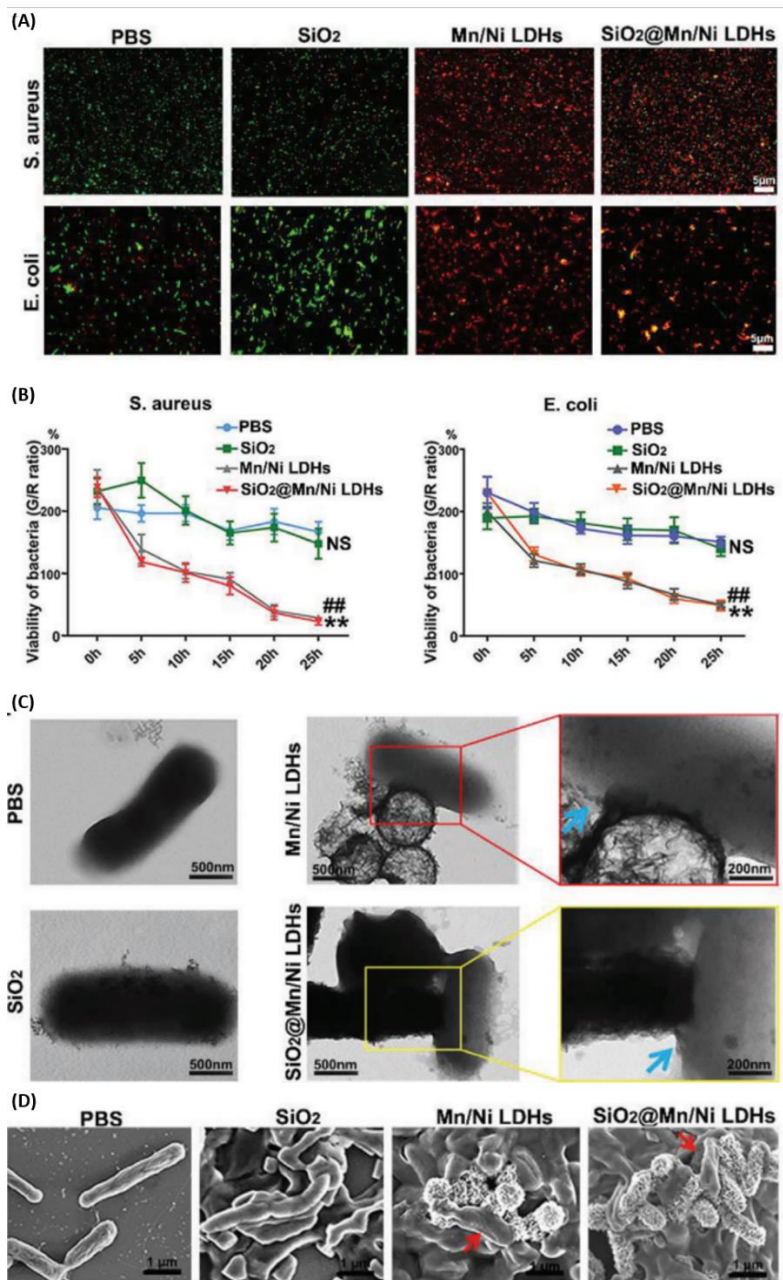
127
 128 **Fig. 2.** Mechanism of *B. subtilis* adhesion onto carbonate intercalated NiFe LDH. (A) Electrostatic
 129 interactions, (B) Anion exchange, (C) OH replacement and (D) H-bond and polar interactions. Reproduced
 130 from Ref. [66] with the permission of Elsevier. Copyright (2013), Elsevier.

131 These mentioned investigations did not correlate the adsorption of bacteria on LDHs to their
 132 antibacterial activity where no antibacterial activity tests were carried out.

133 2.2. Topological adhesion of LDH on bacteria

134 One other possible reason explaining LDH-bacteria adhesion is the rough surface of LDHs thus
 135 promoting the adhesion phenomena which may be a key factor contributing to their antibacterial
 136 activity [45,69]. It had been well known that the motility of bacteria is essential for bacterial normal
 137 functions [70], and that rough antimicrobial colloidal surfaces might adhere to bacteria and disturb
 138 its normal motility functions [71,72]. Zhang *et al.* successfully synthesized antibacterial hybrids
 139 of silica nanorods and unsmooth hollow Mn/Ni LDHs [45]. The antibacterial activities of SiO_2 ,
 140 Mn/Ni LDHs and SiO_2 nanorods @Mn/Ni LDHs were investigated against Gram-negative *E. coli*
 141 and Gram-positive *Staphylococcus aureus* bacteria, by standard cell viability Live/Dead Bac Light
 142 assay (Fig. 3Fig. 3A). The ratio of green (alive bacteria) to red (dead bacteria) fluorescence (G/R)

143 was also measured to compare the antibacterial efficiency of the different tested samples. As
144 shown in **Fig. 3B**, the ratio of G/R fluorescence in both Gram-positive and Gram-negative bacteria
145 decreased significantly over time for hollow Mn/Ni LDHs as well as SiO₂@Mn/Ni LDHs samples,
146 thus indicating their efficient antibacterial activity. The antibacterial activity of Mn/Ni LDHs and
147 SiO₂@Mn/Ni LDHs was related to their bacterial adhesion properties to rough surfaces. As shown
148 in **Fig. 3C and D**, both hollow Mn/Ni LDHs and SiO₂ nanorods@Mn/Ni LDHs exhibited
149 relatively good adhesion (blue arrows) and strong connection (red arrows) with *E.coli*. Therefore,
150 the antibacterial activity of hollow Mn/Ni(OH)_x LDHs structures was attributed to their ability to
151 “seize” the bacteria thus disturbing its motility and leading to its death. Such findings come in line
152 with those of Wang *et al.* who reported the enhancement of antibacterial function by loading
153 lysozyme at the surface of ternary MgZnAl LDHs due to the rough surface of the host flower-like
154 LDH providing better contact with bacteria and thus an amplified antibacterial effect [69]. LDHs
155 adhesion to bacteria could further affect the bacterial biological activities, such as blocking the
156 channels for nutrients uptake and waste exclusion, which would subsequently lead to bacterial
157 death or inhibition [21,47,73]. Moreover, LDHs may also adsorb many essential nutrients for
158 bacterial growth in medium, *e.g.* proteins, celluloses, starch and proteins [21,47]. This would thus
159 reduce the bioavailability of these necessary nutrients and inhibit the bacterial growth.



160

161 **Fig. 3.** (A) Confocal microscopy images of *S. aureus* and *E. coli* incubated with a mixture of propidium
 162 iodide (red color) and SYTO 9 (green color) and various samples. The images correspond to 25 h after
 163 incubation. Green fluorescence corresponds to live bacteria while red fluorescence corresponds to dead
 164 bacteria. (B) The time-dependent concentrations of live bacteria, evaluated by the ratio of G/R. (C) TEM
 165 images of *E. coli* with or without treatment of different samples. Blue arrows correspond to bacterial
 166 adhesion. (D) SEM images of *E. coli* with or without treatment of different samples. Red arrows correspond

167 to a direct connection with *E.coli* bacteria. Reproduced from Ref. [45] with the permission of Wiley Online
168 Library. Copyright (2020), Wiley.

169 Although these investigations suggested that the rough surface of LDHs aid in the adhesion
170 phenomena leading to the achieved antibacterial effect [45,69], real measurements of LDH surface
171 roughness are lacking. One good method to ensure the effectiveness of LDHs roughness in the
172 antibacterial activity is to compare the antibacterial activity of different LDH samples having
173 different surface roughness which could be evaluated easily by atomic force microscopy (AFM)
174 for example [74,75].

175 **2.3. Antibacterial test assays used to evaluate the direct contact antibacterial performance** 176 **of LDHs**

177 Different antibacterial test assays allowed the evaluation antibacterial performance of LDHs
178 associated with direct contact. One very important point to consider while correlating the
179 antibacterial performance of LDHs to their followed antibacterial mechanism is the used
180 antibacterial test assay. Generally, evaluating the antibacterial performance of pristine and NPs-
181 loaded LDHs could be achieved by agar disk or agar well diffusion methods [22,39,40,43,44],
182 plate colony count method [49,76], or else by evaluating the minimum inhibitory concentration
183 (MIC) of LDHs by broth macro or microdilution assays (**Table 1**) [39,40,40,43,58].

184 However, not all assays are suitable to suggest or validate a certain antibacterial mechanism. For
185 instance, Carja *et al.* [39] and Mishra *et al.* [44] suggested direct surface interaction as a
186 mechanism explaining the antibacterial activities of Ag-ZnAl LDH particles. However, they
187 reported inhibitions diameters between 7 and 18 mm in agar-agar gels, which seems in
188 contradiction with a mechanism only driven by contact with the bacteria. Indeed, the mass transfer
189 of particles through convection can be neglected in a gel, therefore the distance run by a particle

190 in those experiments can be estimated with the Fick equation using the Stokes-Einstein equation
191 for the diffusion coefficients [77]. At room temperature, in an agar-agar gel (typical viscosity: $\eta =$
192 0.01 Pa.s or 10 cPl) and with standard LDH particle aggregate (5 μm), the diffusion constant is in
193 the order of magnitude of 4-16 m^2/s . During a standard duration of an experiment of disk diffusion
194 or agar well diffusion (24 to 48h), the typical distance of the particle from the original position is
195 20 to 40 μm . Direct contact cannot be the explanation for the inhibition of the bacterial growth
196 several millimeters away from the place in which LDHs were deposited. Therefore, inhibition zone
197 diameters measurements are not suitable to evaluate the antibacterial effect of LDHs by direct
198 surface interactions.

199 **2.4.Experimental observations, limitation and maximization of the direct contact effect** 200 **of LDHs**

201 Haffner *et al.* investigated the influence of particle size (from 42 to 208 nm) on pristine LDH
202 interactions with bacteria-mimicking membranes (DOPE/DPG) [9]. LDH binding to bacteria-
203 mimicking membranes and their destabilization increased significantly with decreasing particle
204 size. Due to strong interactions with anionic lipopolysaccharide and peptidoglycan layers, direct
205 membrane disruption was observed for both Gram-negative *E. coli* and Gram-positive *S. aureus*
206 bacteria. Such membrane disruption was primarily evidenced by the leakage of the tested
207 membrane liposomes which was enhanced with decreasing LDH particle sizes. The net negative
208 charge of bacteria was also reduced due to the presence of electrostatic surface interactions which
209 were thought to induce the observed membrane disruption.

210 In fact, the influence of LDH particle sizes on their antibacterial properties could also be
211 determined by comparing the MIC values of LDHs having different particle sizes against the same
212 microorganism. For instance, Lobo-Sanchez *et al.* reported a MIC value of 10,000 $\mu\text{g}/\text{mL}$ for bulk

213 Zn-based pristine LDHs (micron-sized agglomerated LDHs) [58], which is remarkably lower than
214 that of ~250 nm-sized Zn-based pristine LDH nanosheets prepared by Dutta *et al.* (MIC value of
215 200 µg/mL) [40]. Moreover, smaller-sized Zn-based LDH nanosheets (~50 nm) investigated by
216 Moaty *et al.* presented even a lower MIC value of 15.6 µg/mL against the same bacterial strain
217 [22]. In this context, LDH nanosheets present a larger surface area and more active sites compared
218 to bulk LDHs. Additionally, the great difference in MIC values between bulk LDHs and LDH
219 nanosheets could also be related to the ability of nanosheets to provide a stable mobile suspension
220 in solution, whereas bulk LDHs tend to sediment, thus limiting the accessible surface and contact
221 with the tested *S. aureus* bacteria.

222 Mao *et al.* designed three different Ag loaded-LDHs composites using three different synthesis
223 methods [61]. **Fig. 4A** shows the transmission electron microscopy (TEM) images of the loaded
224 AgNPs in each composite, the size of loaded Ag-NPs was 25, 65 and 15 nm for Ag-LDHs@TA–
225 Fe(III), Ag-LDHs(PVP) and Ag-LDHs@PDA, respectively. Moreover, the amount of AgNPs
226 loading was determined using energy dispersive spectroscopy (EDS) surface analysis (**Fig. 4B**).
227 Consequently, the antimicrobial performance of the Ag-LDHs hybrids was influenced by both the
228 size and amount of loaded Ag NPs. Ag-LDHs(PVP) hybrid, having the highest Ag loading of
229 3.37% and medium-sized AgNPs, presented the lowest MIC value (**Fig. 4C**), thus being the best
230 tested antimicrobial composite. On the other hand, even with the lowest Ag loading, Ag-
231 LDHs@TA–Fe(III) showed better antibacterial performance than that of Ag-LDHs@PDA, due to
232 its very small particle sizes of loaded AgNPs. A similar finding was reported by Nocchetti *et*
233 *al.*[60], where AgCl-LDH composites with Ag loading of 4.9% and small AgCl NPs (64 nm)
234 showed greater antibacterial performance compared to that of another AgCl-LDH composite with
235 Ag loading of 12.1% but with a larger size (94.8 nm). Therefore, the antibacterial performance

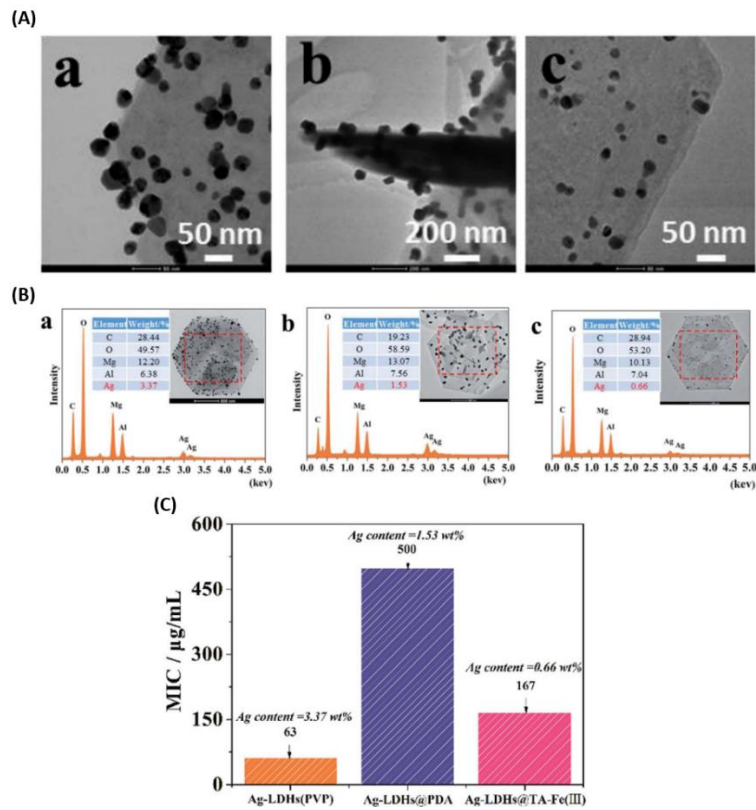
236 was rather dependent on the dimensions of loaded NPs, which corresponded to greater surface area
237 and thereby promoted better contact with the bacteria probably leading to enhanced mobility of
238 NPs adhering to bacteria. In fact, NPs as AgNPs can anchor to the bacterial cell wall and
239 consequently impose membrane damages [78,79]. After adhesion to the bacterial wall, NPs can
240 also penetrate the membrane to interact with cellular structures and biomolecules such as proteins,
241 lipids, and DNA. Interaction between metallic NPs and cellular structures or biomolecules may
242 subsequently lead to bacterial dysfunction and finally growth inhibition or death [78–81]

243 The previously mentioned investigations succeeded to correlate direct surface interactions between
244 bacteria and LDHs to their antibacterial activity. However, the used experimental approaches were
245 only achieved through the evaluation of the effect of LDH particle sizes [9,61] or else through
246 qualitative adhesion observations using SEM or TEM imaging [45,69] without any quantification
247 of the driving forces of interactions. In fact, other methods can be used to investigate and quantify
248 LDHs-bacterial membrane. In this context, the use of recent AFM-based force spectroscopy modes
249 would be helpful, *e.g.* single-molecule and single-cell force spectroscopies (SPFS and SCFS,
250 respectively [82,83]. The use of such force spectroscopy approaches would allow not only a
251 qualitative but also a quantitative evaluation of the presented forces of interactions at the single-
252 particle or single-cell levels.

253 Even though there is still much missing information concerning the role of direct surface
254 interactions in the antibacterial effect of pristine and NPs-loaded LDHs, one could still derive some
255 factors which could help maximize such an effect:

- 256 - an increase in the positive charge of the LDH or the loaded NPs increases the chance of
257 electrostatic interactions with the negatively charged bacterial membranes
- 258 - a rough surface of the LDH promoting adhesion to bacteria

259 - smaller LDH particles or loaded NPs provide enhancing the mobility of the particles and
260 maximumizing surface area for the interaction



261
262 **Fig. 4.** (A) HRTEM images of (a) Ag-LDHs(PVP), (b) Ag-LDHs@PDA and (c) Ag-LDHs@TA–
263 Fe(III). (B): EDS surface scans for (a) Ag-LDHs(PVP), (b) Ag-LDHs@PDA and (c) Ag–
264 LDHs@TA–Fe(III). (C): The MIC values of the different Ag-LDHs against *E. coli*. Reproduced
265 from Ref. [61] with permission from the Royal Society of Chemistry.

266 3. LDH antibacterial activity by dissolution

267 3.1. Release of antibacterial molecules out of antibacterial molecules loaded-LDHs

268 Most investigations highlighting the efficiency of LDHs to act as antibacterial materials were
269 related to their ability to intercalate antibacterial organic biomolecules such as antibiotics
270 [21,47,84], lysozymes [69,85] and antibacterial polymeric organic molecules [86]. This is

271 probably due to LDHs' remarkable property of intercalating a wide variety of anions within their
 272 interlamellar regions. Recently, antibacterial molecules-intercalated LDHs had been also
 273 incorporated with several polymeric matrices to design efficient antibacterial fillers for various
 274 applications as well [87,88]. **Table 2** reports some of the previous work done on the efficiency of
 275 antibacterial compounds-loaded LDH composites.

276 **Table 2.** Antibacterial performance of organic biomolecules-loaded LDHs reported in the literature. MIC
 277 values correspond to the minimum inhibitory concentration required to inhibit the growth of a certain
 278 bacteria, whereas inhibition zone diameters correspond to the obtained inhibitory diameter zone generated
 279 by antimicrobial molecules-loaded LDHs when being tested in agar disk or agar well diffusion tests.

LDH host	Antimicrobial compound	Tested Bacteria	Antibacterial performance	Reference
MgAl	Phenoxymethyl-penicillin	Gram-positive: <i>S. aureus</i>	Penicillin-LDH showed efficient antibacterial activity with inhibition zone diameter ranging from 8 to 25 mm depending on the pH of the media	[84]
ZnAl	Cephazolin	Gram-positive: <i>S. aureus</i>	Cephazolin-LDH possessed an inhibition zone of 225 m ² in water and 240 m ² in presence of 0.8% NaCl	[47]
ZnAl	O-hydroxybenzoate (o-BzOH)	Gram-negative: <i>E. coli</i>	O-BzOH-LDH was able to reduce the growth of bacteria which was evidenced by plate count method. The antimicrobial properties of O-BzOH-LDH were enhanced with decreasing powder dimensions.	[89]
MgAl	Lysozyme (LYZ)	Gram-positive: <i>S. aureus</i>	LYZ-LDHs possessed great antibacterial activity (ranging from 40 to 97.5%) depending on the LYZ/LDH ratio and the pH of the bacteria-containing water	[85]
MgAl	Camphorsulfonic acid, Ciprofloxacin	Gram-positive: <i>S. aureus</i> , <i>S. epidermidis</i> , <i>S. pyogenes</i> Gram-negative: <i>E. coli</i> , <i>Proteus vulgaris</i> , <i>P. aeruginosa</i> , <i>Enterobacter cloacae</i>	Camphorsulfonic acid-LDH composite was active against Gram-negative bacteria with MIC between 1.4 and 10 mg/mL, Ciprofloxacin-LDH was active against both Gram-positive and Gram-negative with higher MIC of 1.3 mg/mL	[90]

MgAl	Turmeric curcuminoid	Gram-positive: <i>S. aureus</i> Gram-negative: <i>E. coli</i> , <i>P. aeruginosa</i>	Curcuminoid-LDH showed inhibition zone diameters against all tested strains ranging from 8 to 19 mm depending on the pH of the medium	[91]
MgAl	Berberine chloride (BBC)	Gram-positive: <i>S. aureus</i> , <i>B. subtilis</i> Gram-negative: <i>P. aeruginosa</i>	BBC-LDH hybrids showed inhibition zone diameters ranging from 2 to 9 mm depending on the type of tested bacteria and applied synthesis method. BBC-LDH hybrid prepared by coprecipitation showed a greater inhibitory effect than that synthesized by anion-exchange.	[92]
MgFeAl	Pipemidic Acid ions	Gram-negative: <i>E. coli</i> , <i>S. typhimurium</i>	Pipemidic acid-LDH showed efficient antimicrobial activity with MIC values of 3.5 and 4.5 mg/mL against <i>E. coli</i> and <i>S. typhimurium</i> , respectively	[93]
ZnAl	Benzoate anions (BZ)	Gram-positive: <i>S. aureus</i>	All hybrid BZ-LDH showed excellent antibacterial activities ensured by plate count method. BZ-LDH prepared by reconstruction route possessed the highest antibacterial activity among the other hybrids prepared by coprecipitation and anion-exchange routes	[94]
ZnAl	Chitosan polymer	Gram-positive: <i>S. aureus</i> , <i>B. subtilis</i> , <i>Lactobacillus sakei</i> , <i>E. faecalis</i> Gram-negative: <i>E. coli</i> , <i>P. aeruginosa</i> , <i>P. vulgaris</i>	Chitosan-LDH had superior activity to that of free chitosan and is active toward <i>L. sakei</i> (MIC=0.125 mg/mL), <i>S. aureus</i> (MIC=0.4 mg/mL), <i>E. coli</i> (MIC=0.2 mg/mL)	[86]
MgAl	3-(4-hydroxyphenyl)propionic acid (HPP) L-ascorbic acid (ASA) L-tyrosine (TYR) L-tryptophan (TRP)	Gram-positive: <i>S. aureus</i> Gram-negative: <i>E. coli</i>	All hybrids except HPP-LDH achieved 100% growth inhibition for both bacteria ensured by plate count method.	[95]
ZnTi	Kojic acid	Gram-positive: <i>S. aureus</i> Gram-negative: <i>E. coli</i> , <i>P. aeruginosa</i>	Kojic acid-LDH was efficient against <i>E. coli</i> and <i>P. aeruginosa</i> with inhibition zone diameters of 10.77 and 6.95 mm, respectively	[96]
CuAl-CMC polymer	Amoxicillin	Gram-positive: <i>S. aureus</i> Gram-negative: <i>E. coli</i>	Amoxicillin-LDH-CMC hybrids showed increasing inhibition zone diameters ranging from 8 to 25 mm depending on the LDH:CMC mass ratio	[87]

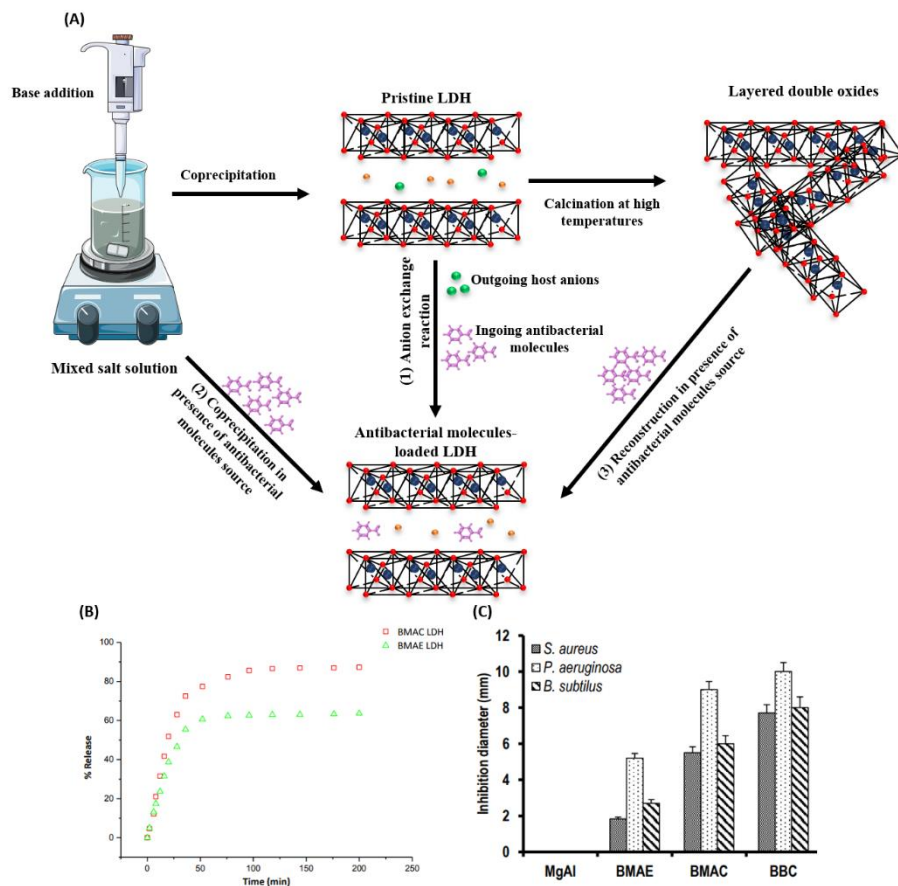
MgAl-LDPE polymer ZnAl-LDPE polymer	Salicylate anions (SA) Rosmarinate anions (RA)	Gram-positive: <i>S. aureus</i> Gram-negative: <i>E. coli</i>	SA-LDH-LDPE and RA-LDH-LDPE hybrids inhibited the growth of both tested bacteria evidenced by plate count method. The highest inhibition was observed for SA-ZnAl-LDPE	[88]
CaAl	Ciprofloxacin	Gram-positive: <i>S. aureus</i> Gram-negative: <i>E. coli</i> , <i>K. pneumoniae</i>	Ciprofloxacin-CaAl hybrids showed an inhibition zone diameter ranging between 43 and 60 mm and MIC values between 0.04 and 0.06 mg/L depending on the type of tested bacteria	[97]

280

281 Nearly all of the studies dealing with the antibacterial activity of antibacterial organic molecules-
 282 loaded LDHs are mainly concerned with the controlled release of the active biomolecule out of the
 283 LDH matrix [31,46,87,93,96,98–100], which is the main contributor to the followed antibacterial
 284 mechanism. . One example of controlled release behavior of antibacterial molecule-loaded LDHs
 285 is the controlled delivery of Kojic acid (KA) out of ZnTi LDH [96]. In phosphate-buffered saline
 286 (PBS, pH = 5), pure KA is released in one step and not gradually. However, the ZnTi-KA
 287 composite released KA anions in a slow gradual manner, where even after 12 h KA anions were
 288 still released. The prolonged release behavior of KA suggests the maintenance of a long-term
 289 antibacterial effect of the LDH hybrid. The long-term antibacterial activity of antimicrobial
 290 molecules loaded-LDHs can be explained by two main reasons: (1) the protection of the LDH
 291 matrix for loaded molecules by isolating them from a hostile environment, (2) the slow release of
 292 loaded molecules from the LDH interlayer [21,46,55]. Moreover, the intercalation of KA into LDH
 293 also improved its stability at higher temperatures. Such enhancement of thermal stability of
 294 antibacterial molecules when being loaded in LDH matrices was also reported in other studies as
 295 well [90,101,102]

296 **3.1.1. Methods for intercalating antibacterial molecules in the LDH and their influence**
 297 **on the release behavior**

298 One important factor influencing the antimicrobial activity of antibacterial molecules-LDH
 299 hybrids is the applied synthesis method [92,94]. As with any other LDH material, antibacterial
 300 molecules loaded-LDHs were prepared by three different methods illustrated in **Fig. 5(A)**: (1)
 301 anion-exchange reactions, (2) direct coprecipitation, (3) rehydration of double layered oxides.



302
 303 **Fig. 5.** (A) Schematic representation of the three different methods used to synthesize antibacterial
 304 molecules-loaded LDHs: (1) Anion-exchange reactions between previously prepared pristine LDHs and
 305 antibacterial molecules basic solution, (2) Direct coprecipitation of mixed metallic salt solutions and base
 306 addition in presence of the antibacterial molecule source, (3) Rehydration of layered double oxides,
 307 previously obtained by calcination of pristine LDHs, in presence of antibacterial molecules source. (B):
 308 Release profiles of BBC from anion exchange and coprecipitation biohybrid LDHs. (C): Inhibitory

309 diameters of free and immobilized BBC. Reproduced from Ref. [92] with permission from Elsevier.
310 Copyright (2016), Elsevier.

311 **(1) Anion exchange reactions:** due to their remarkable property in terms of anion exchange
312 capacity, antibacterial-molecules LDHs can be synthesized by an indirect anion exchange route,
313 which was commonly used for intercalation of larger anions as biological ones for example [103].
314 In this method LDHs with host anions of NO_3^- , CO_3^{2-} , and Cl^- are primarily prepared by
315 coprecipitation, then the exchange with other desired intercalated anions can take place (**Fig. 5A**)
316 [55,104]. In fact, anion-exchange synthesis is the most frequently used method to synthesize
317 antibacterial molecules-intercalated LDHs [32,33,47,90,105].

318 **(2) Coprecipitation:** coprecipitation takes place by the addition of a solution containing the
319 anionic form of the desired antibacterial molecule to be intercalated into another solution having
320 the divalent and trivalent metal cations in a specific ratio. The pH should further be increased by
321 simultaneous addition of a base usually sodium hydroxide (NaOH) or urea hydrolysis that
322 subsequently leads to the precipitation of the antibacterial molecule-intercalated LDH (**Fig. 5A**)
323 [46,84,89]. Although the direct coprecipitation method does not favor the intercalation of large
324 molecules inside the interlamellar space of the LDH [106], several investigations on the synthesis
325 of antibacterial molecules-intercalated LDHs using the coprecipitation method were reported
326 [46,89].

327 **(3) Rehydration of double layer oxides:** one property of LDH clay materials is their ability to
328 regain their original structure back after calcination followed by rehydration, this property is
329 termed as “memory effect” [107]. Calcining LDHs at mild temperatures (400-500°C) would
330 transfer them to their respective layered double oxides by eliminating interlayer water molecules,
331 hydroxyl groups, and previously intercalated anions. Furthermore, when these obtained metal

332 oxides are immersed in another solution containing other anions to be intercalated (antibacterial
333 anions in this case), the LDH structure can be regenerated back by rehydration (Fig. 5A) [108].
334 Several antibacterial molecules were successfully loaded into the LDH interlamellar spacing using
335 this synthesis method [84,109].

336 Djebbi *et al.* compared the antibacterial behavior of the same LDH composite synthesized using
337 two different methods, conventional anion exchange (AE) and direct coprecipitation (AC) routes
338 [92]. The amount of loaded antibacterial molecule berberine chloride (BBC) in the inorganic
339 matrix, estimated by UV-Vis spectroscopy analysis, was found to be 24% and 93% in BMAE and
340 BMAC, respectively. Moreover, the release profiles of BBC from AE and AC biohybrid LDHs
341 were separately measured in PBS at pH = 7.4 (**Fig. 5B**), and the released percentage of BBC from
342 AC was greater than that from AE. Consequently, the antimicrobial activity of AC was more
343 efficient than that of AE (**Fig. 5C**) due to an improvement in chemical stability, the greater amount
344 of loaded and released BBC. On contrary, Mishra *et al.* pointed out the lower antimicrobial
345 efficiency and lower release behavior of Benzoate-LDH hybrids synthesized by coprecipitation in
346 comparison to those synthesized by anion-exchange and reconstruction methods [94]. The authors
347 attributed the difference in the antimicrobial performance of the hybrids synthesized using
348 different methods to the different orientations of benzoate anions within the interlamellar space of
349 the LDH in each case. Such different orientation resulted in a different loading and release behavior
350 of antibacterial molecules as previously suggested by Wang *et al.* [33]. Such contradiction suggests
351 that choosing a particular synthesis method to synthesize antibacterial molecules-loaded LDHs is
352 an important factor to be taken into consideration. Therefore, an optimization of the most efficient
353 synthesis method should be performed according to the type, structure, and orientations of the
354 antibacterial molecules loaded in the LDH interlayer.

355 **3.1.2. Influence of the LDH host on the antibacterial activity of antibacterial molecules-**
356 **loaded LDH composites**

357 Bugatti *et al.* reported the influence of powder dimensions evaluated by granulometry analysis on
358 the antimicrobial properties of antibacterial molecules-loaded LDHs [89]. Antibacterial
359 composites (ZnAl-o-BzOH) based on ZnAl LDH and o-hydroxybenzoate (o-BzOH), also known
360 as salicylate, were synthesized by a direct coprecipitation method. The initial powder dimensions
361 were reduced by the high energy ball milling (HEBM) technique for 1 to 5 min influencing the
362 size as well as the morphology of the powders. Large, agglomerated particles were found for the
363 pristine samples, while well-defined platelets with uniform and thinner sizes were present in the
364 milled samples. The antimicrobial activity against *E. coli* was found much more effective for the
365 samples with lower powder dimensions. Therefore, particles with lower dimensions provided an
366 enhanced release of o-BzOH anions and an enhanced antibacterial activity. A similar finding was
367 suggested by Kuznetsova *et al.* who reported a remarkable impact of the hydrodynamic radius of
368 the LDH composite powders on the release behavior of 2-mercaptobenzothiazole anions out of
369 ZnAl LDH host and therefore an enhanced antibacterial activity [110].

370 Moreover, Coiai *et al.* had recently reported the contribution of the host LDH to the antimicrobial
371 activity of antibacterial molecules-modified LDHs [88], where salicylic acid SA-ZnAl LDH
372 hybrids provided higher antibacterial activity against Gram-negative *E. coli* and Gram-positive *S.*
373 *aureus* bacteria in comparison to SA-MgAl LDH hybrids. The authors attributed the enhanced
374 antibacterial activity of SA-ZnAl to the presence of zinc ions in the structure which may have
375 contributed to the antibacterial performance of the hybrid alongside the antibacterial action of SA.
376 The specific effect of Zn²⁺ ions as an antimicrobial agent will be detailed in **section 3.2.1**. Such

377 synergistic antibacterial effect of Zn^{2+} ions released out ZnAl LDHs and organic molecules loaded
378 in the LDH matrix was also reported by Li *et al.* [21].

379 **3.1.3. Principles for the design of an efficient antibacterial molecules-loaded LDH**

380 When designing antibacterial molecules-loaded LDH composites of controlled release behavior,
381 several factors must be taken into consideration to provide an enhanced antibacterial behavior
382 including:

- 383 - the efficiency of the antibacterial guest molecule itself
- 384 - the synthesis method of the composite and the orientation of antibacterial molecule within
385 the interlamellar spacing of the LDH matrix allowing maximum loading
- 386 - the size and dimensions of the resulted composite controlling the release behavior of the
387 hosted antibacterial biomolecule
- 388 - the type of LDH host matrix aiding in the antibacterial performance

389 **3.2. Dissolution of metallic cations out of pristine and NPs-loaded LDHs**

390 As suggested previously, the release of metallic ions is one other possible mechanism explaining
391 the antibacterial activity of pristine and NPs-loaded LDHs (**Table 1**). Metallic ions as Zn^{2+} , Cu^{2+}
392 and Ag^+ can damage bacterial membrane functions by: (i) blocking the transport of nutrients and
393 substances in and out of the membrane, (ii) reducing protein and enzymatic expressions, (iii) or
394 else by binding to bacterial intracellular DNA leading to their denaturation [73,111–114].

395 **3.2.1. Antimicrobial effect through the release of Zn^{2+} , Cu^{2+} and Ag^+**

396 Moaty *et al.* reported an efficient antibacterial activity against several Gram-positive and Gram-
397 negative bacterial strains for ZnFe pristine LDH which was slightly weaker than that imposed by
398 standard antibiotics [22]. The authors suggested that released zinc ions had a great effect on both

399 bacteria because of the binding to their membranes which prolonged the lag phase of the growth
400 cycle. Dutta *et al.* also reported a significant impact of Zn₂Al-CO₃ LDH on several Gram-positive
401 and Gram-negative bacteria. The antibacterial efficiency varied in accordance with the applied
402 dosage of Zn₂Al-CO₃ LDH, where it was greatly enhanced for growing concentrations.
403 Additionally, the antibacterial activity was also dependent on the type of tested bacteria. Among
404 the tested microorganisms, Gram-negative bacteria were comparatively more sensitive toward the
405 LDH sample than Gram-positive ones. The authors reported that released Zn²⁺ could strongly
406 contribute to the observed antibacterial effect. Finally, the difference in the antibacterial activity
407 between Gram-negative and Gram-positive bacteria was clarified by the different structures and
408 the chemical composition of the cell surfaces of these two types of bacteria. Gram-positive bacteria
409 possess an extra outer membrane that covers the peptidoglycan layer that is not present in Gram-
410 negative bacteria [115].

411 Vallejo *et al.* reported the influence of the nature and amount of constituent divalent metal on the
412 antibacterial activity of pristine LDHs [116]. LDH samples containing copper or magnesium as
413 divalent metals were found to be less active against *Corynebacterium ammoniagenes*, whereas
414 those containing zinc showed superior bactericidal activity ranging from 98.1% to 99.9%
415 depending on the applied dosage. The reason behind the enhanced activity of Zn-based LDHs was
416 linked to the superior efficiency of the released zinc ions to induce an antibacterial effect than
417 other released ions as Cu²⁺ and Mg²⁺. The impact of the nature of constituent divalent metal was
418 also reported by Li *et al.* who studied the antibacterial activity of different MAI-LDH (M: Mg²⁺,
419 Cu²⁺, Ni²⁺, Co²⁺, and Mn²⁺) against Gram-negative *E. coli*, and *S. aureus* Gram-positive bacteria.
420 When the concentration of MAI-LDHs increased up to 1500 µg/mL, CuAl-LDH and MnAl-LDH
421 showed the best bacterial inhibition compared to the other LDH samples. On the other hand, NiAl-

422 LDH and CoAl-LDH exhibited a limited antibacterial activity, whereas MgAl-LDH had no
423 antibacterial ability. Similarly, Peng *et al.* compared the antimicrobial activity of MgAl and MgFe
424 LDHs to those of ZnAl and ZnFe LDHs, where the two latter presented superior antibacterial
425 properties [73]. A global investigation of the impact of different released constituent divalent
426 metallic cations of MAI-LDHs (M: Mg²⁺, Cu²⁺, Ni²⁺, Co²⁺, and Zn²⁺) was also performed recently
427 by our group [43], where it was found out that only Cu and Zn-based LDHs releasing Cu²⁺ and
428 Zn²⁺ ions were able to impose an efficient antibacterial effect against *S. aureus* and *E. coli* bacteria.
429 The inhibition zone diameters of all LDH samples were very similar to those of their corresponding
430 metallic salts counterparts (having a concentration similar to that of the one released by LDHs,
431 thus suggesting the strong relation between the antibacterial activity of pristine LDHs and their
432 metallic ions release capacity. Additionally, we figured out that not only the nature of constituent
433 divalent metals could impact the antibacterial effect of pristine LDH but also the stability and
434 crystallinity of LDHs. For instance, exchanging carbonate anions with other anions having lower
435 intercalating affinities as Cl⁻, NO₃⁻ and ClO₄⁻, increasing the Zn(II):Al(III) molar ratio [43,58] and
436 lowering the crystallinity enhanced the release of Zn²⁺ in aqueous broth media and subsequently
437 the showed greater inhibition zone diameters and lower MIC values.

438 Tabti *et al.* synthesized a range of Cu-LDHs having different molar ratios of Cu:Al (Cu_{0.05}–
439 Al_{0.15}, Cu_{0.10}–Al_{0.10}, Cu_{0.14}–Al_{0.06}, and Cu_{0.15}–Al_{0.05}) [42]. The antibacterial activity of
440 the synthesized samples was estimated toward several bacterial strains, e.g. *E. coli*, *P. aeruginosa*,
441 *E. faecalis*, *S. aureus*, and *B. Subtilis*. Samples having a higher molar ratio of Cu:Al showed better
442 antibacterial activity due to the presence of a greater amount of Cu²⁺ ions which were further
443 ejected providing an enhanced impact.

444 Huang *et al.* reported the fabrication of hybrid polypyrrole-silver coated layered double hydroxides
445 (LDHs@PPy-Ag) for both enhanced gas carrier property and antibacterial activity [117]. The
446 prepared LDH hybrid was able to completely inhibit the growth of bacteria. The antibacterial
447 activity of the prepared LDH hybrid was attributed to the synergistic effect of polypyrrole and the
448 loaded silver NPs. In particular, it was believed that the direct contact effect with loaded AgNPs
449 alongside the Ag⁺ ions released from unstable AgNPs were responsible for the excellent observed
450 antibacterial activity.

451 Yadollahi *et al.* prepared antibacterial nanocomposite hydrogels by the combination of
452 carboxymethyl cellulose (CMC), LDH and silver nanoparticles (AgNPs) [118]. CMC-LDH
453 hydrogels were prepared by intercalating CMC into different LDHs, *e.g.* MgAl, NiAl, CuAl and
454 ZnAl LDHs. Ag/CMC-LDH nanocomposite hydrogels (Ag/CMC-Mg-LDH, Ag/CMC-Ni-LDH,
455 Ag/CMC-Cu-LDH and Ag/CMC-Zn-LDH) were prepared through *in situ* formation of AgNPs
456 within the CMC-LDHs. CMC-Mg-LDH and CMC-Ni-LDH showed no antibacterial activity
457 against *E. coli* and *S. aureus*. On contrary, an antibacterial effect was observed for both CMC-Cu-
458 LDH and CMC-Zn-LDH nanocomposites. Such an effect was attributed to the antibacterial
459 features of Cu²⁺ and Zn²⁺ ions released from CMC-Cu-LDH and CMC-Zn-LDH nanocomposites,
460 respectively. Ag/CMC-LDH nanohybrids exhibited a superior antibacterial activity against both
461 bacteria in comparison to their CMC-LDH counterparts. The authors attributed such enhanced
462 antibacterial activity to the antibacterial effect of released Ag⁺ ions from Ag/CMC-LDH
463 nanohybrids. Metal ions were slowly released from metallic NPs as AgNPs, and then absorbed
464 through the cell membrane. The released silver metallic ions were probably able to interact with
465 functional groups of nucleic acids and proteins, *e.g.* mercapto (-SH), amino (-NH), carboxyl (-
466 COOH) groups [119]. This could further affect the normal physiological processes by damaging

467 the enzymatic activity, changing the cell structure, and ultimately inhibiting the growth of
468 microorganisms [81,119].

469 **3.2.2. Correlation to the amount of metallic ions released and principles for the design**
470 **of LDHs with optimal antibacterial effect through ion release**

471 Although all the previously mentioned investigations suggest the contribution of released metallic
472 ions to the antibacterial effect of pristine and NPs-loaded LDHs, the literature lacks real
473 experimental setups validating such contribution, *e.g.* quantitative evaluation of the concentration
474 of released ions in solution and their antibacterial efficiency. In our study [51], the MIC values of
475 Zn-based LDHs were studied in accordance with the amount of zinc ions released in LB and TSB
476 broth media. The MIC values of Zn-based LDHs decreased significantly from 12 to 0.375 mg/mL
477 when higher amounts of zinc ions were released. Therefore, we were able to establish the
478 contribution of metallic ions released out of pristine LDHs to their antibacterial properties thus
479 confirming the suggested antibacterial mechanism of metallic ions release.

480 In summary, several properties of pristine and NPs-loaded LDHs can be tuned in a way that the
481 antibacterial effect by metallic ions release could be enhanced, including:

- 482 - nature of constituent divalent metal or loaded NP to be released, *e.g.* Zn²⁺, Cu²⁺ and Ag⁺,
483 having the greater effect
- 484 - increasing the release of the divalent cations in various ways:
 - 485 ○ increasing the divalent to the trivalent metal molar ratio of LDH (M^{II}:M^{III})
 - 486 ○ lowering the crystallinity of LDH powders
 - 487 ○ introducing intercalating anions having lower affinity to the layers

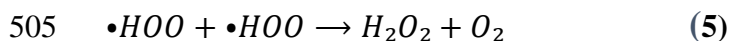
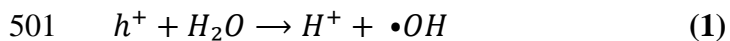
- 488 ○ decreasing the size of LDHs or loaded NPs which could provide an impact on the
- 489 amount of metallic ions released, *e.g.* smaller particles release more metallic ions
- 490 - tuning the amount and stability of loaded NPs for NPs-loaded LDHs

491 **4. LDH antibacterial activity by the generation of reactive oxygen species**

492 Reactive oxygen species (ROS) are produced by bacteria itself (endogenous) as a byproduct of
 493 aerobic respiration or generated in the host environment (exogenous) [120]. ROS were called
 494 “double-edged swords of life” in the mechanism of pathogen clearance [121]. First, successful
 495 pathogens can exploit endogenous ROS for their growth and adaption. Second, exogenous ROS
 496 were thought to be the weapon providing an efficient antibacterial effect since they can directly
 497 damage bacterial membranes, DNA, lipids, and proteins by oxidative stress [120–122].

498 **4.1. Generation of ROS by LDHs**

499 When a suitable source of light irradiates LDHs, an electron (\bar{e}) and a hole (h^+) are created which
 500 could subsequently generate ROS by the following reactions [123]:



506 Where $\bullet OH$ are hydroxyl radicals, $\bullet O_2^-$ are superoxide radical anions, $\bullet HOO$ are hydrogen
 507 superoxide radicals, and H_2O_2 are hydrogen peroxide molecules, all belonging to the family of

508 ROS. The generation of ROS by LDHs is another possible mechanism explaining their
509 antibacterial activity as suggested by several studies reported in **Table 1**.

510 **4.2. ROS generation by pristine LDHs**

511 Zhao *et al.* reported the synthesis of antibacterial ZnTi LDH nanosheets with lateral dimensions in
512 the range of 40–80 nm [124]. ESR and X-ray photoelectron spectroscopy (XPS) measurements
513 revealed that Ti^{3+} sites were generated within these nanosized LDH platelets. The antibacterial
514 activity of ZnTi LDHs found upon visible-light illumination was explained by the generation of
515 superoxide anion radicals ($\bullet O_2^-$) and hydroxyl radicals by trapping of electrons by Ti^{3+} ions and
516 the reaction of generated holes with water or hydroxyl ions ($\bullet OH$), respectively. These generated
517 ROS ($\bullet O_2^-$ and $\bullet OH$) were believed to be strong and nonselective oxidants, which could lead to the
518 damage of bacteria by attacking cell membrane to cause cell lysis.

519 **4.3. ROS generation by supported nanoparticles on LDH**

520 **4.3.1. Ag@AgCl-generated ROS**

521 Nocchetti *et al.* successfully synthesized antibacterial LDH hybrids by loading AgCl NPs on ZnAl
522 LDHs for Rhodamine B (RhB) dye photodegradation and antibacterial potential applications [60].
523 Kinetic experiments of the antibacterial activity of the prepared hybrids in the dark and under
524 irradiation ($\lambda > 350$ nm). No bacterial growth reduction was observed until 180 min upon treatment
525 with LDH hybrids in dark conditions. On the other hand, the number of live bacteria treated with
526 LDH hybrids was considerably reduced after 60 min of irradiation. The superior antibacterial
527 activity of the nanocomposites under irradiation for a very short time was explained by the
528 formation of Ag clusters on AgCl and the production of reactive oxygen species (ROS), such as
529 $\bullet O_2^-$, which was previously observed in the photodegradation process of RhB in presence of ROS
530 quenchers.

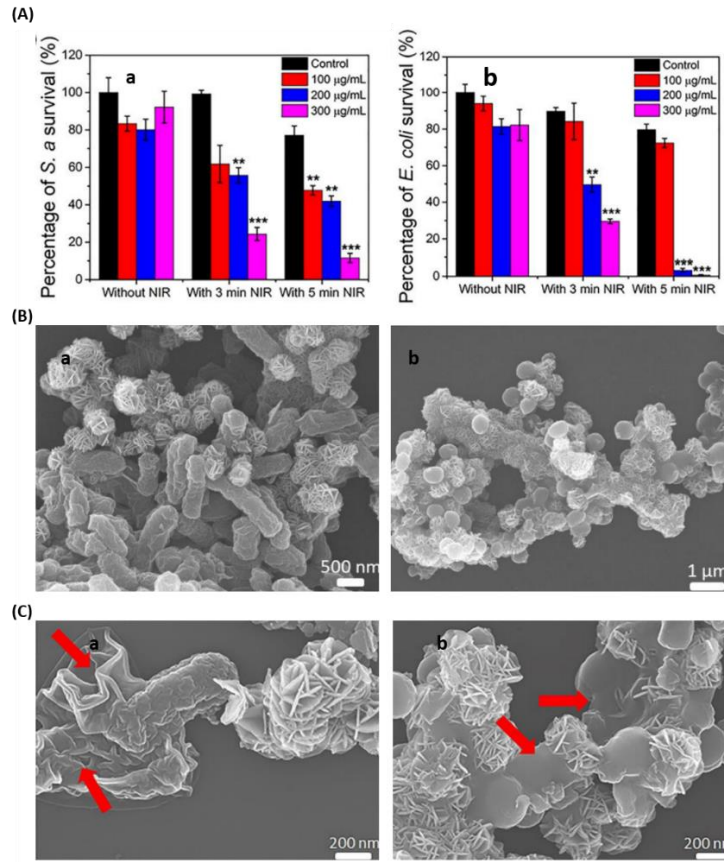
531 **4.3.2. ZnO-generated ROS**

532 Zhang *et al.* reported the fabrication of antibacterial nanocomposites based on loading zinc oxides
533 NPs (ZnO) on ZnAl LDHs which were further incorporated in water polyurethane (WPU)
534 polymeric matrix [49]. The antibacterial activities of the pure WPU, WPU/ZnAl-LDHs and
535 WPU/ZnO-loaded ZnAl-LDHs composite films with different ZnAl-LDHs/ZnO contents were
536 tested against *E. coli* and *S. aureus*. It was noted that the pure WPU did not show any antibacterial
537 activity, while the WPU/ZnAl-LDHs showed a weak antibacterial property. However, the
538 WPU/ZnO-loaded ZnAl-LDHs composites showed a strong antibacterial activity which reached
539 99% at a very low loading of 0.3 wt%. The authors explained the enhanced antibacterial property
540 of WPU/ZnO-loaded ZnAl-LDHs composites as follows: ZnO is a semiconductor with a wide
541 bandgap, which could be stimulated by photon energy higher than the bandgap of ZnO (3.37 eV),
542 and could lead to the movement of an electron from the valence band (V_b) to the conduction band
543 (C_b) of the particle. Thus, a hole (h^+) in the valence band and a free electron (e^-) in the conduction
544 band would be generated, triggering reactions (1)-(5) described in **section 4.1**. This in turn would
545 damage the bacterial cells. Similar suggested antibacterial mechanism concerning the generation
546 of ROS by ZnO-loaded ZnAl LDHs was also reported by Li *et al.* [125]. This mechanism was also
547 cited for layered double oxides containing those types of oxide species as well [42,76].

548 **4.3.3. Beyond ROS: photothermal effect of Au on LDHs**

549 Ma *et al.* reported the construction of an antibacterial core-shell gold nanorods-loaded LDHs
550 (GNR@LDH) nanostructures by loading gold nanorods (GNR) on a MgAl LDH matrix [38]. As
551 shown in **Fig. 6A**, the antibacterial activity of the synthesized GNR@LDH nanostructures showed
552 significant antibacterial activity against *E. coli* and *S. aureus* bacteria, only when being irradiated
553 by Near Infrared (NIR) laser ($\lambda=808$ nm). When the concentration exceeded 200 $\mu\text{g/mL}$,

554 GNR@LDH-PEG exhibited a significant antibacterial effect in 3 minutes of irradiation and even
555 a higher effect (99.25% and 88.44% for *E.coli* and *S. aureus*, respectively). Moreover, the SEM
556 images shown in **Fig. 6B** and **C** revealed that both bacteria adhered to GNR@LDH nanostructures,
557 probably due to their positively charged surface. However, before being irradiated by 808 nm laser,
558 no obvious damages were detected on the bacterial membrane of the rod-shaped *E. coli* and
559 spherical *S. aureus* (**Fig. 6B**). On the contrary, under irradiation with a NIR laser for 3 minutes,
560 some crumbles appeared on the surface and the cell membranes became incomplete, distorted, and
561 even melted (**Fig. 6C**, red arrows). Such observation suggested that bacterial adhesion to LDH
562 nanostructures is not responsible for their antibacterial effect, but it rather served as a first step in
563 promoting the antibacterial activity, as previously suggested by Gottenbos *et al.* [64]. In summary,
564 GNR@LDH showed remarkable photothermal antibacterial activity on both Gram-positive and
565 Gram-negative bacteria. This consequently led to the damage and destruction of *E. coli* and *S.*
566 *aureus* bacterial membranes.



567

568 **Fig. 6.** (A) Antibacterial activity evaluation of GNR@LDH-PEG against: (a) *E. coli*, (b): *S. aureus*. (B)
 569 SEM images of treated bacteria with GNR@LDH without 808 nm laser: (a) *E. coli*, (b) *S. aureus*. (C) SEM
 570 images of bacteria treated with GNR@LDH under 3 min irradiation with 808 nm laser: (a) *E. coli*, (b) *S.*
 571 *aureus*; * $P < 0.01$, $0.001 < **P < 0.005$, *** $P < 0.001$, compared with control group, red arrows correspond
 572 to distorted cell membranes. Reproduced with permission from Ref. [38]. Copyright (2019), American
 573 Chemical Society.

574 It is somehow difficult to determine whether the observed damaged bacterial membranes were
 575 indeed due to the generation of ROS or the reported photothermal activity under irradiation. To
 576 validate such a hypothesis, the morphology of irradiated untreated bacteria should be examined as
 577 well.

578 **4.4.Limitation of the attribution of the ROS mechanism and general considerations for**
579 **its effect**

580 The aforementioned studies suggested either the contribution of ROS [41,42,49,58,60,76] or the
581 photothermal effect [38] to the antibacterial mechanism of pristine and NPs-loaded LDHs. A real
582 measurement of ROS and the evaluation of their role is therefore necessary to distinguish the
583 contribution of each to the antibacterial activity. ROS generation could be evaluated using different
584 methods including fluorescence spectroscopy using fluorescent dye probes, ESR and
585 chromatography methods [126].

586 Another helpful suggestion to ensure the contribution of the generation of ROS by LDHs to their
587 antibacterial activity is to study the antibacterial effect of LDHs in function of generated ROS
588 initially evaluated using both qualitative and quantitative approaches. For example, Dutta *et al.*
589 confirmed that the antibacterial effect of ZnO NPs was related to bacterial membrane damage
590 caused by generated ROS evaluated using fluorescent dye probes [127]. Additionally, a scavenger
591 of ROS (histidine) was also used in different concentrations during antibacterial experiments in
592 order to evaluate more precisely the role of the generated ROS in the adapted antibacterial
593 mechanism. The antibacterial activity of ZnO NPs decreased significantly with increasing
594 concentrations of added histidine thus ensuring the great contribution of generated ROS to the
595 antibacterial performance of ZnO NPs.

596 In summary, ROS generation had been evidenced only for pristine LDHs (ZnTi LDH nanosheets).
597 The possibilities for ROS generation are increased with nanoparticle loading, either with metallic
598 particles (Au), halogen-metal salts (AgCl) or oxides (ZnO).

599 ROS generation should be triggered by UV, visible or IR light. Of course, a reference measurement
600 must be performed to ensure that the light source itself does not contribute to the observed
601 antibacterial effect.

602 **5. Conclusion**

603 As summarized in this review, LDH-based materials, *e.g.*, pristine LDHs, NPs loaded-LDHs and
604 antibacterial molecules-loaded LDHs, could be potentially used as efficient antibacterial agents
605 against various Gram-positive and Gram-negative bacterial strains.

606 (1) Direct surface interactions between negatively charged bacterial membranes and positively
607 charged pristine or NPs-loaded LDHs constitute one possible mechanism explaining their
608 antibacterial activity. Such interaction is maximized by substantial surface charges, smaller
609 particle sizes and good dispersion of LDHs or loaded NPs to promote better interaction
610 with bacterial membranes leading to their damage.

611 (2) Dissolution of antibacterial molecules from antibacterial molecules-loaded LDH
612 composites is believed to be the main contributor to their antibacterial effect. The induced
613 antibacterial effect by the controlled release of loaded antibacterial molecules is dependent
614 on the efficiency and amount of the loaded antibacterial molecules, their orientation within
615 the LDH matrix, the size of the composites controlling the dissolution behavior as well as
616 the nature of the LDH host which could also aid in the antibacterial effect of these
617 composites. Moreover, dissolution also occurs for pristine and NPs-loaded LDHs that
618 partially release their constituent divalent metallic ions (especially Zn^{2+} and Cu^{2+}) and NPs
619 metallic ions (Ag^+), respectively. The release behavior of these metallic ions is dependent
620 on several factors and is increased for lower crystallinity of the particles, weakly
621 interacting intercalated anions, larger divalent over trivalent ion ratio. The released metallic

622 ions can further cause damages to the membrane functions by blocking the transport of
623 nutrients and substances in and out the membrane, or by binding to bacterial intracellular
624 DNA and proteins leading to their denaturation or deactivation.

625 (3) Finally, upon being radiated by a suitable source of illumination, pristine (Ti-Zn LDH) as
626 well as NPs-loaded (Ag@AgCl, ZnO and Au) LDHs can generate reactive oxygen species
627 (ROS) such as $\bullet\text{HO}$, $\bullet\text{O}_2^-$ and H_2O_2 . These generated ROS are well known to be toxic to
628 bacteria by which they can damage their bacterial membranes, DNA, lipids, and proteins
629 by oxidative stress.

630 Although these different mechanisms were proposed to explain the antibacterial mode of action
631 of LDH-based materials, experimental evidences verifying them are still lacking. Hence,
632 special investigations are highly encouraged to study in detail the antibacterial mechanisms of
633 LDH-based materials. So that they could potentially be utilized as antibacterial agents in
634 different fields of applications such as antibacterial coatings, food packaging products, cement
635 additives, wound healing and textiles products.

636 **Acknowledgment**

637 The authors acknowledge the financial support from the French Ministry of Higher Education
638 (MESR), the French National Scientific Centre (CNRS).

639 **References**

- 640 [1] M.C. Fitzpatrick, C.T. Bauch, J.P. Townsend, A.P. Galvani, Modelling microbial infection
641 to address global health challenges, *Nat. Microbiol.* 4 (2019) 1612–1619.
642 <https://doi.org/10.1038/s41564-019-0565-8>.
643 [2] A. Chatterjee, J. Abraham, Microbial Contamination, Prevention, and Early Detection in
644 Food Industry, in: *Microb. Contam. Food Degrad.*, Elsevier, 2018: pp. 21–47.
645 <https://doi.org/10.1016/B978-0-12-811515-2.00002-0>.

- 646 [3] Md.S. Rahman, Md.I.H. Mondal, Md.S. Hasan, J. Alom, M.B. Ahmed, F. Ahmed,
647 Microorganisms, infection and the role of medical textiles, in: *Antimicrob. Text. Nat.*
648 *Resour.*, Elsevier, 2021: pp. 45–85. <https://doi.org/10.1016/B978-0-12-821485-5.00004-4>.
- 649 [4] A.M.G.A. Laheij, J.O. Kistler, G.N. Belibasakis, H. Välimaa, J.J. de Soet, *European Oral*
650 *Microbiology Workshop (EOMW) 2011, Healthcare-associated viral and bacterial*
651 *infections in dentistry*, *J. Oral Microbiol.* 4 (2012) 17659.
652 <https://doi.org/10.3402/jom.v4i0.17659>.
- 653 [5] M.E. Eissa, *Distribution of bacterial contamination in non-sterile pharmaceutical materials*
654 *and assessment of its risk to the health of the final consumers quantitatively*, *Beni-Suef*
655 *Univ. J. Basic Appl. Sci.* 5 (2016) 217–230. <https://doi.org/10.1016/j.bjbas.2016.08.005>.
- 656 [6] E. Christaki, M. Marcou, A. Tofarides, *Antimicrobial Resistance in Bacteria: Mechanisms,*
657 *Evolution, and Persistence*, *J. Mol. Evol.* 88 (2020) 26–40. [https://doi.org/10.1007/s00239-
658 *019-09914-3*.](https://doi.org/10.1007/s00239-019-09914-3)
- 659 [7] C. Nathan, *Resisting antimicrobial resistance*, *Nat. Rev. Microbiol.* 18 (2020) 259–260.
660 <https://doi.org/10.1038/s41579-020-0348-5>.
- 661 [8] C. Forano, F. Bruna, C. Mousty, V. Prevot, *Interactions between Biological Cells and*
662 *Layered Double Hydroxides: Towards Functional Materials*, *Chem. Rec.* 18 (2018) 1150–
663 1166. <https://doi.org/10.1002/tcr.201700102>.
- 664 [9] S. Malekhaat Häffner, M. Malmsten, *Membrane interactions and antimicrobial effects of*
665 *inorganic nanoparticles*, *Adv. Colloid Interface Sci.* 248 (2017) 105–128.
666 <https://doi.org/10.1016/j.cis.2017.07.029>.
- 667 [10] C. Wang, P. Makvandi, E.N. Zare, F.R. Tay, L. Niu, *Advances in Antimicrobial Organic*
668 *and Inorganic Nanocompounds in Biomedicine*, *Adv. Ther.* 3 (2020) 2000024.
669 <https://doi.org/10.1002/adtp.202000024>.
- 670 [11] R. Kumar, A. Umar, G. Kumar, H.S. Nalwa, *Antimicrobial properties of ZnO*
671 *nanomaterials: A review*, *Ceram. Int.* 43 (2017) 3940–3961.
672 <https://doi.org/10.1016/j.ceramint.2016.12.062>.
- 673 [12] S. Kim, J. Fahel, P. Durand, E. André, C. Carteret, *Ternary Layered Double Hydroxides*
674 *(LDHs) Based on Co-, Cu-Substituted ZnAl for the Design of Efficient Photocatalysts:*
675 *Ternary Layered Double Hydroxides (LDHs) Based on Co-, Cu-Substituted ZnAl for the*
676 *Design of Efficient Photocatalysts*, *Eur. J. Inorg. Chem.* 2017 (2017) 669–678.
677 <https://doi.org/10.1002/ejic.201601213>.
- 678 [13] A. Razzaq, S. Ali, M. Asif, S.-I. In, *Layered Double Hydroxide (LDH) Based*
679 *Photocatalysts: An Outstanding Strategy for Efficient Photocatalytic CO₂ Conversion,*
680 *Catalysts.* 10 (2020) 1185. <https://doi.org/10.3390/catal10101185>.
- 681 [14] A.-L. Johnston, E. Lester, O. Williams, R.L. Gomes, *Understanding Layered Double*
682 *Hydroxide properties as sorbent materials for removing organic pollutants from*
683 *environmental waters*, *J. Environ. Chem. Eng.* 9 (2021) 105197.
684 <https://doi.org/10.1016/j.jece.2021.105197>.
- 685 [15] O. Williams, I. Clark, R.L. Gomes, T. Perehinec, J.L. Hobman, D.J. Stekel, R. Hyde, C.
686 Dodds, E. Lester, *Removal of copper from cattle footbath wastewater with layered double*
687 *hydroxide adsorbents as a route to antimicrobial resistance mitigation on dairy farms*, *Sci.*
688 *Total Environ.* 655 (2019) 1139–1149. <https://doi.org/10.1016/j.scitotenv.2018.11.330>.
- 689 [16] S. Yang, M. Liu, F. Deng, L. Mao, S. Yu, H. Huang, J. Chen, L. Liu, X. Zhang, Y. Wei, A
690 novel fluorescent DNA sensor system based on polydopamine modified MgAl-layered

- 691 double hydroxides, *Colloid Interface Sci. Commun.* 37 (2020) 100294.
692 <https://doi.org/10.1016/j.colcom.2020.100294>.
- 693 [17] X. Bi, H. Zhang, L. Dou, Layered Double Hydroxide-Based Nanocarriers for Drug
694 Delivery, *Pharmaceutics*. 6 (2014) 298–332.
695 <https://doi.org/10.3390/pharmaceutics6020298>.
- 696 [18] S. Senapati, R. Thakur, S.P. Verma, S. Duggal, D.P. Mishra, P. Das, T. Shripathi, M. Kumar,
697 D. Rana, P. Maiti, Layered double hydroxides as effective carrier for anticancer drugs and
698 tailoring of release rate through interlayer anions, *J. Controlled Release*. 224 (2016) 186–
699 198. <https://doi.org/10.1016/j.jconrel.2016.01.016>.
- 700 [19] B. Ballarin, A. Mignani, F. Mogavero, S. Gabbanini, M. Morigi, Hybrid material based on
701 ZnAl hydrotalcite and silver nanoparticles for deodorant formulation, *Appl. Clay Sci.* 114
702 (2015) 303–308. <https://doi.org/10.1016/j.clay.2015.06.014>.
- 703 [20] A. Donnadio, M. Bini, C. Centracchio, M. Mattarelli, S. Caponi, V. Ambrogi, D. Pietrella,
704 A. Di Michele, R. Vivani, M. Nocchetti, Bioinspired Reactive Interfaces Based on Layered
705 Double Hydroxides-Zn Rich Hydroxyapatite with Antibacterial Activity, *ACS Biomater.*
706 *Sci. Eng.* 7 (2021) 1361–1373. <https://doi.org/10.1021/acsbiomaterials.0c01643>.
- 707 [21] M. Li, Y. Sultanbawa, Z.P. Xu, W. Gu, W. Chen, J. Liu, G. Qian, High and long-term
708 antibacterial activity against *Escherichia coli* via synergy between the antibiotic penicillin
709 G and its carrier ZnAl layered double hydroxide, *Colloids Surf. B Biointerfaces*. 174 (2019)
710 435–442. <https://doi.org/10.1016/j.colsurfb.2018.11.035>.
- 711 [22] S.A.A. Moaty, A.A. Farghali, R. Khaled, Preparation, characterization and antimicrobial
712 applications of Zn-Fe LDH against MRSA, *Mater. Sci. Eng. C*. 68 (2016) 184–193.
713 <https://doi.org/10.1016/j.msec.2016.05.110>.
- 714 [23] L. Mohapatra, K. Parida, A review on the recent progress, challenges and perspective of
715 layered double hydroxides as promising photocatalysts, *J. Mater. Chem. A*. 4 (2016) 10744–
716 10766. <https://doi.org/10.1039/C6TA01668E>.
- 717 [24] P. Nalawade, B. Aware, V.J. Kadam, R.S. Hirlekar, Layered double hydroxides: A review,
718 *Layer. DOUBLE HYDROXIDES*. 68 (2009) 6.
- 719 [25] Vicente Rives, *Layered double hydroxides: Present and Future*, New York, 2001.
- 720 [26] F.L. Theiss, G.A. Ayoko, R.L. Frost, Synthesis of layered double hydroxides containing
721 Mg²⁺, Zn²⁺, Ca²⁺ and Al³⁺ layer cations by co-precipitation methods—A review, *Appl.*
722 *Surf. Sci.* 383 (2016) 200–213. <https://doi.org/10.1016/j.apsusc.2016.04.150>.
- 723 [27] F. Cavani, F. Trifirò, A. Vaccari, Hydrotalcite-type anionic clays: Preparation, properties
724 and applications., *Catal. Today*. 11 (1991) 173–301. [https://doi.org/10.1016/0920-](https://doi.org/10.1016/0920-5861(91)80068-K)
725 [5861\(91\)80068-K](https://doi.org/10.1016/0920-5861(91)80068-K).
- 726 [28] P. Dutta, S. Auerbach, K. Carrad, *Handbook of Layered Materials*, CRC Press, 2004.
727 <https://doi.org/10.1201/9780203021354>.
- 728 [29] N.B. Allou, P. Saikia, A. Borah, R.L. Goswamee, Hybrid nanocomposites of layered double
729 hydroxides: an update of their biological applications and future prospects, *Colloid Polym.*
730 *Sci.* 295 (2017) 725–747. <https://doi.org/10.1007/s00396-017-4047-3>.
- 731 [30] L. Yan, S. Gonca, G. Zhu, W. Zhang, X. Chen, Layered double hydroxide nanostructures
732 and nanocomposites for biomedical applications, *J. Mater. Chem. B*. 7 (2019) 5583–5601.
733 <https://doi.org/10.1039/C9TB01312A>.
- 734 [31] S.B. Khan, K. Alamry, N. Alyahyawi, A. Asiri, Controlled release of
735 organic–inorganic nanohybrid: cefadroxil intercalated Zn–Al-layered double

- hydroxide, Int. J. Nanomedicine. Volume 13 (2018) 3203–3222.
https://doi.org/10.2147/IJN.S138840.
- [32] G. Mishra, B. Dash, D. Sethi, S. Pandey, B.K. Mishra, Orientation of Organic Anions in Zn-Al Layered Double Hydroxides with Enhanced Antibacterial Property, Environ. Eng. Sci. 34 (2017) 516–527. https://doi.org/10.1089/ees.2016.0531.
- [33] Y. Wang, D. Zhang, Synthesis, characterization, and controlled release antibacterial behavior of antibiotic intercalated Mg–Al layered double hydroxides, Mater. Res. Bull. 47 (2012) 3185–3194. https://doi.org/10.1016/j.materresbull.2012.08.029.
- [34] U. Bogdanović, V. Lazić, V. Vodnik, M. Budimir, Z. Marković, S. Dimitrijević, Copper nanoparticles with high antimicrobial activity, Mater. Lett. 128 (2014) 75–78. https://doi.org/10.1016/j.matlet.2014.04.106.
- [35] T.C. Dakal, A. Kumar, R.S. Majumdar, V. Yadav, Mechanistic Basis of Antimicrobial Actions of Silver Nanoparticles, Front. Microbiol. 7 (2016). https://doi.org/10.3389/fmicb.2016.01831.
- [36] M.M. Mohamed, S.A. Fouad, H.A. Elshoky, G.M. Mohammed, T.A. Salaheldin, Antibacterial effect of gold nanoparticles against *Corynebacterium pseudotuberculosis*, Int. J. Vet. Sci. Med. 5 (2017) 23–29. https://doi.org/10.1016/j.ijvsm.2017.02.003.
- [37] R. Pati, R.K. Mehta, S. Mohanty, A. Padhi, M. Sengupta, B. Vaseeharan, C. Goswami, A. Sonawane, Topical application of zinc oxide nanoparticles reduces bacterial skin infection in mice and exhibits antibacterial activity by inducing oxidative stress response and cell membrane disintegration in macrophages, Nanomedicine Nanotechnol. Biol. Med. 10 (2014) 1195–1208. https://doi.org/10.1016/j.nano.2014.02.012.
- [38] K. Ma, Y. Li, Z. Wang, Y. Chen, X. Zhang, C. Chen, H. Yu, J. Huang, Z. Yang, X. Wang, Z. Wang, Core–Shell Gold Nanorod@Layered Double Hydroxide Nanomaterial with Highly Efficient Photothermal Conversion and Its Application in Antibacterial and Tumor Therapy, ACS Appl. Mater. Interfaces. 11 (2019) 29630–29640. https://doi.org/10.1021/acsami.9b10373.
- [39] G. Carja, Y. Kameshima, A. Nakajima, C. Dranca, K. Okada, Nanosized silver–anionic clay matrix as nanostructured ensembles with antimicrobial activity, Int. J. Antimicrob. Agents. 34 (2009) 534–539. https://doi.org/10.1016/j.ijantimicag.2009.08.008.
- [40] S. Dutta, T.K. Jana, S.K. Halder, R. Maiti, A. Dutta, A. Kumar, K. Chatterjee, Zn₂Al–CO₃ Layered Double Hydroxide: Adsorption, Cytotoxicity and Antibacterial Performances, ChemistrySelect. 5 (2020) 6162–6171. https://doi.org/10.1002/slct.202001264.
- [41] M. Li, L. Li, S. Lin, Efficient antimicrobial properties of layered double hydroxide assembled with transition metals via a facile preparation method, Chin. Chem. Lett. 31 (2020) 1511–1515. https://doi.org/10.1016/j.ccllet.2019.09.047.
- [42] H.A. Tabti, M. Adjdir, A. Ammam, B. Mdjahed, B. Guezzen, A. Ramdani, C.K. Bendeddouche, N. Bouchikhi, N. Chami, Facile synthesis of Cu-LDH with different Cu/Al molar ratios: application as antibacterial inhibitors, Res. Chem. Intermed. 46 (2020) 5377–5390. https://doi.org/10.1007/s11164-020-04268-8.
- [43] J. Awassa, D. Cornu, S. Soulé, C. Carteret, C. Ruby, S. El-Kirat-Chatel, Divalent metal release and antimicrobial effects of layered double hydroxides, Appl. Clay Sci. 216 (2022) 106369. https://doi.org/10.1016/j.clay.2021.106369.
- [44] G. Mishra, B. Dash, S. Pandey, P.P. Mohanty, Antibacterial actions of silver nanoparticles incorporated Zn–Al layered double hydroxide and its spinel, J. Environ. Chem. Eng. 1 (2013) 1124–1130. https://doi.org/10.1016/j.jece.2013.08.031.

- 782 [45] W. Zhang, Y. Zhao, W. Wang, J. Peng, Y. Li, Y. Shanguan, G. Ouyang, M. Xu, S. Wang,
783 J. Wei, H. Wei, W. Li, Z. Yang, Colloidal Surface Engineering: Growth of Layered Double
784 Hydroxides with Intrinsic Oxidase-Mimicking Activities to Fight Against Bacterial
785 Infection in Wound Healing, *Adv. Healthc. Mater.* 9 (2020) 2000092.
786 <https://doi.org/10.1002/adhm.202000092>.
- 787 [46] M.A. Djebbi, A. Elabed, Z. Bouaziz, M. Sadiki, S. Elabed, P. Namour, N. Jaffrezic-Renault,
788 A.B.H. Amara, Delivery system for berberine chloride based on the nanocarrier ZnAl-
789 layered double hydroxide: Physicochemical characterization, release behavior and
790 evaluation of anti-bacterial potential, *Int. J. Pharm.* 515 (2016) 422–430.
791 <https://doi.org/10.1016/j.ijpharm.2016.09.089>.
- 792 [47] S.-J. Ryu, H. Jung, J.-M. Oh, J.-K. Lee, J.-H. Choy, Layered double hydroxide as novel
793 antibacterial drug delivery system, *J. Phys. Chem. Solids.* 71 (2010) 685–688.
794 <https://doi.org/10.1016/j.jpcs.2009.12.066>.
- 795 [48] M. Nocchetti, A. Donnadio, V. Ambrogi, P. Andreani, M. Bastianini, D. Pietrella, L.
796 Latterini, Ag/AgCl nanoparticle decorated layered double hydroxides: synthesis,
797 characterization and antimicrobial properties, *J. Mater. Chem. B.* 1 (2013) 2383.
798 <https://doi.org/10.1039/c3tb00561e>.
- 799 [49] W.-D. Zhang, Y.-M. Zheng, Y.-S. Xu, Y.-X. Yu, Q.-S. Shi, L. Liu, H. Peng, Y. Ouyang,
800 Preparation and Antibacterial Property of Waterborne Polyurethane/Zn–Al Layered Double
801 Hydroxides/ZnO Nanocomposites, *J. Nanosci. Nanotechnol.* 13 (2013) 409–416.
802 <https://doi.org/AG>.
- 803 [50] M.V. Bukhtiyarova, A review on effect of synthesis conditions on the formation of layered
804 double hydroxides, *J. Solid State Chem.* 269 (2019) 494–506.
805 <https://doi.org/10.1016/j.jssc.2018.10.018>.
- 806 [51] D. Chaillot, S. Bennici, J. Brendlé, Layered double hydroxides and LDH-derived materials
807 in chosen environmental applications: a review, *Environ. Sci. Pollut. Res.* 28 (2021) 24375–
808 24405. <https://doi.org/10.1007/s11356-020-08498-6>.
- 809 [52] N. Chubar, R. Gilmour, V. Gerda, M. Mičušík, M. Omastova, K. Heister, P. Man, J.
810 Fraissard, V. Zaitsev, Layered double hydroxides as the next generation inorganic anion
811 exchangers: Synthetic methods versus applicability, *Adv. Colloid Interface Sci.* 245 (2017)
812 62–80. <https://doi.org/10.1016/j.cis.2017.04.013>.
- 813 [53] Q. Wang, D. O’Hare, Recent Advances in the Synthesis and Application of Layered Double
814 Hydroxide (LDH) Nanosheets, *Chem. Rev.* 112 (2012) 4124–4155.
815 <https://doi.org/10.1021/cr200434v>.
- 816 [54] G. Mishra, B. Dash, S. Pandey, Layered double hydroxides: A brief review from
817 fundamentals to application as evolving biomaterials, *Appl. Clay Sci.* 153 (2018) 172–186.
818 <https://doi.org/10.1016/j.clay.2017.12.021>.
- 819 [55] V. Rives, M. del Arco, C. Martín, Intercalation of drugs in layered double hydroxides and
820 their controlled release: A review, *Appl. Clay Sci.* 88–89 (2014) 239–269.
821 <https://doi.org/10.1016/j.clay.2013.12.002>.
- 822 [56] R. Sharma, G.G.C. Arizaga, A.K. Saini, P. Shandilya, Layered double hydroxide as
823 multifunctional materials for environmental remediation: from chemical pollutants to
824 microorganisms, *Sustain. Mater. Technol.* 29 (2021) e00319.
825 <https://doi.org/10.1016/j.susmat.2021.e00319>.
- 826 [57] P.D. Marcato, N.V. Parizotto, D.S.T. Martinez, A.J. Paula, I.R. Ferreira, P.S. Melo, N.
827 Durán, O.L. Alves, New Hybrid Material Based on Layered Double Hydroxides and

- 828 Biogenic Silver Nanoparticles: Antimicrobial Activity and Cytotoxic Effect, *J. Braz. Chem.*
829 *Soc.* 24 (2013) 266–272. <https://doi.org/10.5935/0103-5053.20130034>.
- 830 [58] M. Lobo-Sánchez, G. Nájera-Meléndez, G. Luna, V. Segura-Pérez, J.A. Rivera, G. Fetter,
831 ZnAl layered double hydroxides impregnated with eucalyptus oil as efficient hybrid
832 materials against multi-resistant bacteria, *Appl. Clay Sci.* 153 (2018) 61–69.
833 <https://doi.org/10.1016/j.clay.2017.11.017>.
- 834 [59] G. Mishra, B. Dash, S. Pandey, D. Sethi, Ternary layered double hydroxides (LDH) based
835 on Cu- substituted Zn Al for the design of efficient antibacterial ceramics, *Appl. Clay Sci.*
836 165 (2018) 214–222. <https://doi.org/10.1016/j.clay.2018.08.021>.
- 837 [60] M. Nocchetti, M. Pica, B. Ridolfi, A. Donnadio, E. Boccalon, G. Zampini, D. Pietrella, M.
838 Casciola, AgCl-ZnAl Layered Double Hydroxides as Catalysts with Enhanced
839 Photodegradation and Antibacterial Activities, *Inorganics.* 7 (2019) 120.
840 <https://doi.org/10.3390/inorganics7100120>.
- 841 [61] L. Mao, J. Liu, S. Zheng, H. Wu, Y. Liu, Z. Li, Y. Bai, Mussel-inspired nano-silver loaded
842 layered double hydroxides embedded into a biodegradable polymer matrix for enhanced
843 mechanical and gas barrier properties, *RSC Adv.* 9 (2019) 5834–5843.
844 <https://doi.org/10.1039/C8RA09602C>.
- 845 [62] V.P. Harden, J.O. Harris, THE ISOELECTRIC POINT OF BACTERIAL CELLS, *J.*
846 *Bacteriol.* 65 (1953) 198–202. <https://doi.org/10.1128/jb.65.2.198-202.1953>.
- 847 [63] W.W. Wilson, M.M. Wade, S.C. Holman, F.R. Champlin, Status of methods for assessing
848 bacterial cell surface charge properties based on zeta potential measurements, *J. Microbiol.*
849 *Methods.* 43 (2001) 153–164. [https://doi.org/10.1016/S0167-7012\(00\)00224-4](https://doi.org/10.1016/S0167-7012(00)00224-4).
- 850 [64] B. Gottenbos, D.W. Grijpma, H.C. Van der Mei, J. Feijen, H.J. Busscher, Antimicrobial
851 effects of positively charged surfaces on adhering Gram-positive and Gram-negative
852 bacteria, *J. Antimicrob. Chemother.* 48 (2001) 7–13. <https://doi.org/10.1093/jac/48.1.7>.
- 853 [65] Z.P. Xu, G.S. Stevenson, C.-Q. Lu, G.Q. (Max) Lu, P.F. Bartlett, P.P. Gray, Stable
854 Suspension of Layered Double Hydroxide Nanoparticles in Aqueous Solution, *J. Am.*
855 *Chem. Soc.* 128 (2006) 36–37. <https://doi.org/10.1021/ja056652a>.
- 856 [66] J. Liu, C. Duan, J. Zhou, X. Li, G. Qian, Z.P. Xu, Adsorption of bacteria onto layered double
857 hydroxide particles to form biogranule-like aggregates, *Appl. Clay Sci.* 75–76 (2013) 39–
858 45. <https://doi.org/10.1016/j.clay.2013.02.007>.
- 859 [67] S. Miyata, Anion-Exchange Properties of Hydrotalcite-Like Compounds, *Clays Clay Miner.*
860 31 (1983) 305–311. <https://doi.org/10.1346/CCMN.1983.0310409>.
- 861 [68] S. Jin, P.H. Fallgren, J.M. Morris, Q. Chen, Removal of bacteria and viruses from waters
862 using layered double hydroxide nanocomposites, *Sci. Technol. Adv. Mater.* 8 (2007) 67–
863 70. <https://doi.org/10.1016/j.stam.2006.09.003>.
- 864 [69] Z. Wang, H. Yu, K. Ma, Y. Chen, X. Zhang, T. Wang, S. Li, X. Zhu, X. Wang, Flower-like
865 Surface of Three-Metal-Component Layered Double Hydroxide Composites for Improved
866 Antibacterial Activity of Lysozyme, *Bioconjug. Chem.* 29 (2018) 2090–2099.
867 <https://doi.org/10.1021/acs.bioconjchem.8b00305>.
- 868 [70] E. Tamar, M. Koler, A. Vaknin, The role of motility and chemotaxis in the bacterial
869 colonization of protected surfaces, *Sci. Rep.* 6 (2016) 19616.
870 <https://doi.org/10.1038/srep19616>.
- 871 [71] H. Song, Y. Ahmad Nor, M. Yu, Y. Yang, J. Zhang, H. Zhang, C. Xu, N. Mitter, C. Yu,
872 Silica Nanopollens Enhance Adhesion for Long-Term Bacterial Inhibition, *J. Am. Chem.*
873 *Soc.* 138 (2016) 6455–6462. <https://doi.org/10.1021/jacs.6b00243>.

- 874 [72] W. Yan, L. Yang, H. Wang, J. Zhang, W. Shen, Atomic-engineered gold@silvergold alloy
875 nanoflowers for *in vivo* inhibition of bacteria, *Nanoscale*. 10 (2018) 15661–15668.
876 <https://doi.org/10.1039/C8NR04196B>.
- 877 [73] F. Peng, D. Wang, D. Zhang, H. Cao, X. Liu, The prospect of layered double hydroxide as
878 bone implants: A study of mechanical properties, cytocompatibility and antibacterial
879 activity, *Appl. Clay Sci.* 165 (2018) 179–187. <https://doi.org/10.1016/j.clay.2018.08.020>.
- 880 [74] Z. Yu, X. Li, Y. Peng, X. Min, D. Yin, L. Shao, MgAl-Layered-Double-Hydroxide/Sepiolite
881 Composite Membrane for High-Performance Water Treatment Based on Layer-by-Layer
882 Hierarchical Architectures, *Polymers*. 11 (2019) 525.
883 <https://doi.org/10.3390/polym11030525>.
- 884 [75] H.-J. Kim, S.H. Kim, H.-M. Kim, Y.S. Kim, J.-M. Oh, Surface roughness effect on the
885 cellular uptake of layered double hydroxide nanoparticles, *Appl. Clay Sci.* 202 (2021)
886 105992. <https://doi.org/10.1016/j.clay.2021.105992>.
- 887 [76] Y. Qiao, Q. Li, H. Chi, M. Li, Y. Lv, S. Feng, R. Zhu, K. Li, Methyl blue adsorption
888 properties and bacteriostatic activities of Mg-Al layer oxides via a facile preparation
889 method, *Appl. Clay Sci.* 163 (2018) 119–128. <https://doi.org/10.1016/j.clay.2018.07.018>.
- 890 [77] H.B. Drugeon, M.E. Juvin, J. Caillon, A.L. Courtieu, Assessment of formulas for calculating
891 critical concentration by the agar diffusion method, *Antimicrob. Agents Chemother.* 31
892 (1987) 870–875. <https://doi.org/10.1128/AAC.31.6.870>.
- 893 [78] B. Khalandi, N. Asadi, M. Milani, S. Davaran, A. Abadi, E. Abasi, A. Akbarzadeh, A
894 Review on Potential Role of Silver Nanoparticles and Possible Mechanisms of their Actions
895 on Bacteria, *Drug Res.* 67 (2016) 70–76. <https://doi.org/10.1055/s-0042-113383>.
- 896 [79] Y. Qing, L. Cheng, R. Li, G. Liu, Y. Zhang, X. Tang, J. Wang, H. Liu, Y. Qin, Potential
897 antibacterial mechanism of silver nanoparticles and the optimization of orthopedic implants
898 by advanced modification technologies, *Int. J. Nanomedicine*. Volume 13 (2018) 3311–
899 3327. <https://doi.org/10.2147/IJN.S165125>.
- 900 [80] M. Godoy-Gallardo, U. Eckhard, L.M. Delgado, Y.J.D. de Roo Puente, M. Hoyos-Nogués,
901 F.J. Gil, R.A. Perez, Antibacterial approaches in tissue engineering using metal ions and
902 nanoparticles: From mechanisms to applications, *Bioact. Mater.* 6 (2021) 4470–4490.
903 <https://doi.org/10.1016/j.bioactmat.2021.04.033>.
- 904 [81] E. Sánchez-López, D. Gomes, G. Esteruelas, L. Bonilla, A.L. Lopez-Machado, R. Galindo,
905 A. Cano, M. Espina, M. Ettcheto, A. Camins, A.M. Silva, A. Durazzo, A. Santini, M.L.
906 Garcia, E.B. Souto, Metal-Based Nanoparticles as Antimicrobial Agents: An Overview,
907 *Nanomaterials*. 10 (2020) 292. <https://doi.org/10.3390/nano10020292>.
- 908 [82] A. Beaussart, S. El-Kirat-Chatel, Microbial adhesion and ultrastructure from the single-
909 molecule to the single-cell levels by Atomic Force Microscopy, *Cell Surf.* 5 (2019) 100031.
910 <https://doi.org/10.1016/j.tcs.2019.100031>.
- 911 [83] A. Beaussart, C. Feuillie, S. El-Kirat-Chatel, The microbial adhesive arsenal deciphered by
912 atomic force microscopy, *Nanoscale*. 12 (2020) 23885–23896.
913 <https://doi.org/10.1039/D0NR07492F>.
- 914 [84] W.-Z. Li, J. Lu, J.-S. Chen, G.-D. Li, Y.-S. Jiang, L.-S. Li, B.-Q. Huang,
915 Phenoxymethylpenicillin-intercalated hydrotalcite as a bacteria inhibitor, *J. Chem. Technol.*
916 *Biotechnol.* 81 (2006) 89–93. <https://doi.org/10.1002/jctb.1362>.
- 917 [85] Q.-Z. Yang, Y.-Y. Chang, H.-Z. Zhao, Preparation and antibacterial activity of lysozyme
918 and layered double hydroxide nanocomposites, *Water Res.* 47 (2013) 6712–6718.
919 <https://doi.org/10.1016/j.watres.2013.09.002>.

- 920 [86] W. Kamal, W.M.A. El Rouby, A.O. El-Gendy, A.A. Farghali, Bimodal applications of
921 LDH-chitosan nanocomposite: water treatment and antimicrobial activity, IOP Conf. Ser.
922 Mater. Sci. Eng. 464 (2018) 012005. <https://doi.org/10.1088/1757-899X/464/1/012005>.
- 923 [87] S. Behzadi Nia, M. Pooresmaeil, H. Namazi, Carboxymethylcellulose/layered double
924 hydroxides bio-nanocomposite hydrogel: A controlled amoxicillin nanocarrier for colonic
925 bacterial infections treatment, Int. J. Biol. Macromol. 155 (2020) 1401–1409.
926 <https://doi.org/10.1016/j.ijbiomac.2019.11.115>.
- 927 [88] S. Coiai, F. Cicogna, S. Pinna, R. Spiniello, M. Onor, W. Oberhauser, M.-B. Coltelli, E.
928 Passaglia, Antibacterial LDPE-based nanocomposites with salicylic and rosmarinic acid-
929 modified layered double hydroxides, Appl. Clay Sci. 214 (2021) 106276.
930 <https://doi.org/10.1016/j.clay.2021.106276>.
- 931 [89] V. Bugatti, L. Esposito, L. Franzetti, L. Tamaro, V. Vittoria, Influence of the powder
932 dimensions on the antimicrobial properties of modified layered double hydroxide, Appl.
933 Clay Sci. 75–76 (2013) 46–51. <https://doi.org/10.1016/j.clay.2013.02.017>.
- 934 [90] B. Kutlu, P. Schröttner, A. Leuteritz, R. Boldt, E. Jacobs, G. Heinrich, Preparation of melt-
935 spun antimicrobially modified LDH/polyolefin nanocomposite fibers, Mater. Sci. Eng. C.
936 41 (2014) 8–16. <https://doi.org/10.1016/j.msec.2014.04.021>.
- 937 [91] A. Megalathan, S. Kumarage, A. Dilhari, M.M. Weerasekera, S. Samarasinghe, N.
938 Kottegoda, Natural curcuminoids encapsulated in layered double hydroxides: a novel
939 antimicrobial nanohybrid, Chem. Cent. J. 10 (2016) 35. <https://doi.org/10.1186/s13065-016-0179-7>.
- 940 [92] M.A. Djebbi, Z. Bouaziz, A. Elabed, M. Sadiki, S. Elabed, P. Namour, N. Jaffrezic-Renault,
941 A.B.H. Amara, Preparation and optimization of a drug delivery system based on berberine
942 chloride-immobilized MgAl hydrotalcite, Int. J. Pharm. 506 (2016) 438–448.
943 <https://doi.org/10.1016/j.ijpharm.2016.04.048>.
- 944 [93] A. Santana-Cruz, J.L. Flores-Moreno, R. Guerra-González, M.D.J. Martínez-Ortiz,
945 Antibacterial Activity of Pipemidic Acid ions-MgFeAl Layered Double Hydroxide Hybrid
946 Against *E. coli* and *S. typhi*, J. Mex. Chem. Soc. 60 (2017).
947 <https://doi.org/10.29356/jmcs.v60i2.74>.
- 948 [94] G. Mishra, B. Dash, S. Pandey, D. Sethi, C.G. Kumar, Comparative Evaluation of Synthetic
949 Routes and Antibacterial/Antifungal Properties of Zn–Al Layered Double Hydroxides
950 Containing Benzoate Anion, Environ. Eng. Sci. 35 (2018) 247–260.
951 <https://doi.org/10.1089/ees.2017.0062>.
- 952 [95] G. Totaro, L. Sisti, A. Celli, I. Aloisio, D. Di Gioia, A.A. Marek, V. Verney, F. Leroux,
953 Dual chain extension effect and antibacterial properties of biomolecules interleaved within
954 LDH dispersed into PBS by *in situ* polymerization, Dalton Trans. 47 (2018) 3155–3165.
955 <https://doi.org/10.1039/C7DT03914J>.
- 956 [96] X.-R. Wang, H.-M. Cheng, X.-W. Gao, W. Zhou, S.-J. Li, X.-L. Cao, D. Yan, Intercalation
957 assembly of kojic acid into Zn-Ti layered double hydroxide with antibacterial and whitening
958 performances, Chin. Chem. Lett. 30 (2019) 919–923.
959 <https://doi.org/10.1016/j.ccllet.2019.03.050>.
- 960 [97] M.L. Jadam, S.A. Syed Mohamad, H.M. Zaki, Z. Jubri, S.H. Sarijo, Antibacterial activity
961 and physicochemical characterization of calcium-aluminium-ciprofloxacin-layered double
962 hydroxide, J. Drug Deliv. Sci. Technol. 62 (2021) 102314.
963 <https://doi.org/10.1016/j.jddst.2020.102314>.
- 964

- 965 [98] A. Imran, S. López-Rayó, J. Magid, H.C.B. Hansen, Dissolution kinetics of pyroaurite-type
966 layered double hydroxide doped with Zn: Perspectives for pH controlled micronutrient
967 release, *Appl. Clay Sci.* 123 (2016) 56–63. <https://doi.org/10.1016/j.clay.2015.12.016>.
- 968 [99] J.P. Raval, D.R. Naik, K.A. Amin, P.S. Patel, Controlled-release and antibacterial studies
969 of doxycycline-loaded poly(ϵ -caprolactone) microspheres, *J. Saudi Chem. Soc.* 18 (2014)
970 566–573. <https://doi.org/10.1016/j.jscs.2011.11.004>.
- 971 [100] Y. Wang, D. Zhang, Q. Bao, J. Wu, Y. Wan, Controlled drug release characteristics and
972 enhanced antibacterial effect of graphene oxide–drug intercalated layered double hydroxide
973 hybrid films, *J. Mater. Chem.* 22 (2012) 23106. <https://doi.org/10.1039/c2jm35144g>.
- 974 [101] Z. Geng, W. Zhen, Preparation, characterization, structure-property relationships, and
975 thermal degradation kinetics of poly (lactic acid)/amidated potassium hydrogen phthalate
976 intercalated layered double hydroxides nanocomposites, *Polym. Adv. Technol.* 30 (2019)
977 504–518. <https://doi.org/10.1002/pat.4486>.
- 978 [102] C. Madhusa, K. Rajapaksha, I. Munaweera, M. de Silva, C. Perera, G. Wijesinghe, M.
979 Weerasekera, D. Attygalle, C. Sandaruwan, N. Kottegoda, A Novel Green Approach to
980 Synthesize Curcuminoid-Layered Double Hydroxide Nanohybrids: Adroit Biomaterials for
981 Future Antimicrobial Applications, *ACS Omega.* 6 (2021) 9600–9608.
982 <https://doi.org/10.1021/acsomega.1c00151>.
- 983 [103] U. Costantino, R. Vivani, M. Bastianini, F. Costantino, M. Nocchetti, Ion exchange and
984 intercalation properties of layered double hydroxides towards halide anions, *Dalton Trans.*
985 43 (2014) 11587–11596. <https://doi.org/10.1039/C4DT00620H>.
- 986 [104] L.P.F. Benício, R.A. Silva, J.A. Lopes, D. Eulálio, R.M.M. dos Santos, L.A. de Aquino, L.
987 Vergütz, R.F. Novais, L.M. da Costa, F.G. Pinto, J. Tronto, LAYERED DOUBLE
988 HYDROXIDES: NANOMATERIALS FOR APPLICATIONS IN AGRICULTURE, *Rev.*
989 *Bras. Ciênc. Solo.* 39 (2015) 1–13. <https://doi.org/10.1590/01000683rbcs2015081>.
- 990 [105] U. Costantino, V. Bugatti, G. Gorrasi, F. Montanari, M. Nocchetti, L. Tammara, V. Vittoria,
991 New Polymeric Composites Based on Poly(ϵ -caprolactone) and Layered Double
992 Hydroxides Containing Antimicrobial Species, *ACS Appl. Mater. Interfaces.* 1 (2009) 668–
993 677. <https://doi.org/10.1021/am8001988>.
- 994 [106] J. Das, K.M. Parida, Heteropoly acid intercalated Zn/Al HTlc as efficient catalyst for
995 esterification of acetic acid using n-butanol, *J. Mol. Catal. Chem.* 264 (2007) 248–254.
996 <https://doi.org/10.1016/j.molcata.2006.09.033>.
- 997 [107] J. Rocha, M. del Arco, V. Rives, M.A. Ulibarri, Reconstruction of layered double
998 hydroxides from calcined precursors: a powder XRD and ^{27}Al MAS NMR study, *J. Mater.*
999 *Chem.* 9 (1999) 2499–2503. <https://doi.org/10.1039/a903231b>.
- 1000 [108] K.L. Erickson, T.E. Bostrom, R.L. Frost, A study of structural memory effects in synthetic
1001 hydrotalcites using environmental SEM, *Mater. Lett.* 59 (2005) 226–229.
1002 <https://doi.org/10.1016/j.matlet.2004.08.035>.
- 1003 [109] J. Wang, Q. Liu, G. Zhang, Z. Li, P. Yang, X. Jing, M. Zhang, T. Liu, Z. Jiang, Synthesis,
1004 sustained release properties of magnetically functionalized organic–inorganic materials:
1005 Amoxicillin anions intercalated magnetic layered double hydroxides via calcined precursors
1006 at room temperature, *Solid State Sci.* 11 (2009) 1597–1601.
1007 <https://doi.org/10.1016/j.solidstatesciences.2009.06.015>.
- 1008 [110] A. Kuznetsova, P.M. Domingues, T. Silva, A. Almeida, M.L. Zheludkevich, J. Tedim,
1009 M.G.S. Ferreira, A. Cunha, Antimicrobial activity of 2-mercaptobenzothiazole released

1010 from environmentally friendly nanostructured layered double hydroxides, *J. Appl.*
1011 *Microbiol.* 122 (2017) 1207–1218. <https://doi.org/10.1111/jam.13433>.

1012 [111] G. Borkow, J. Gabbay, Copper as a Biocidal Tool, *Curr. Med. Chem.* 12 (2005) 2163–2175.
1013 <https://doi.org/10.2174/0929867054637617>.

1014 [112] S. Mittapally, R. Taranum, S. Parveen, Metal ions as antibacterial agents, *J. Drug Deliv.*
1015 *Ther.* 8 (2018) 411–419. <https://doi.org/10.22270/jddt.v8i6-s.2063>.

1016 [113] T. Ishida, Antibacterial mechanism of Ag⁺ ions for bacteriolyses of bacterial cell walls via
1017 peptidoglycan autolysins, and DNA damages, *MOJ Toxicol.* 4 (2018).
1018 <https://doi.org/10.15406/mojt.2018.04.00125>.

1019 [114] S. Midori-Ku, Comparative Bacteriolytic Mechanism for Ag⁺ and Zn²⁺ Ions against
1020 *Staphylococcus Aureus* and *Escherichia Coli*: A review, *Escherichia Coli.* (2019) 12.

1021 [115] P. Amornpitoksuk, S. Suwanboon, S. Sangkanu, A. Sukhoom, J. Wudtipan, K. Srijan, S.
1022 Kaewtaro, Synthesis, photocatalytic and antibacterial activities of ZnO particles modified
1023 by diblock copolymer, *Powder Technol.* 212 (2011) 432–438.
1024 <https://doi.org/10.1016/j.powtec.2011.06.028>.

1025 [116] A.M. León-Vallejo, F.D. Velázquez-Herrera, Á. Sampieri, G. Landeta-Cortés, G. Fetter,
1026 Study of layered double hydroxides as bactericidal materials against *Corynebacterium*
1027 *ammoniagenes*, a bacterium responsible for producing bad odors from human urine and skin
1028 infections, *Appl. Clay Sci.* 180 (2019) 105194. <https://doi.org/10.1016/j.clay.2019.105194>.

1029 [117] H. Huang, Multifunctional Polypyrrole-silver Coated Layered Double Hydroxides
1030 Embedded into a Biodegradable Polymer Matrix for Enhanced Antibacterial and Gas
1031 Barrier Properties, (2019) 11. <https://doi.org/10.12162/jbb.v4i4.015>.

1032 [118] M. Yadollahi, H. Namazi, M. Aghazadeh, Antibacterial carboxymethyl cellulose/Ag
1033 nanocomposite hydrogels cross-linked with layered double hydroxides, *Int. J. Biol.*
1034 *Macromol.* 79 (2015) 269–277. <https://doi.org/10.1016/j.ijbiomac.2015.05.002>.

1035 [119] L. Wang, C. Hu, L. Shao, The antimicrobial activity of nanoparticles: present situation and
1036 prospects for the future, *Int. J. Nanomedicine.* Volume 12 (2017) 1227–1249.
1037 <https://doi.org/10.2147/IJN.S121956>.

1038 [120] H. Li, X. Zhou, Y. Huang, B. Liao, L. Cheng, B. Ren, Reactive Oxygen Species in Pathogen
1039 Clearance: The Killing Mechanisms, the Adaption Response, and the Side Effects, *Front.*
1040 *Microbiol.* 11 (2021) 622534. <https://doi.org/10.3389/fmicb.2020.622534>.

1041 [121] R. Mittler, ROS Are Good, *Trends Plant Sci.* 22 (2017) 11–19.
1042 <https://doi.org/10.1016/j.tplants.2016.08.002>.

1043 [122] B. Ezraty, A. Gennaris, F. Barras, J.-F. Collet, Oxidative stress, protein damage and repair
1044 in bacteria, *Nat. Rev. Microbiol.* 15 (2017) 385–396.
1045 <https://doi.org/10.1038/nrmicro.2017.26>.

1046 [123] H. Abdolmohammad-Zadeh, M. Zamani-Kalajahi, In situ generation of H₂O₂ by a layered
1047 double hydroxide as a visible light nano-photocatalyst: Application to bisphenol A
1048 quantification, *Microchem. J.* 158 (2020) 105303.
1049 <https://doi.org/10.1016/j.microc.2020.105303>.

1050 [124] Y. Zhao, C.J. Wang, W. Gao, B. Li, Q. Wang, L. Zheng, M. Wei, D.G. Evans, X. Duan, D.
1051 O'Hare, Synthesis and antimicrobial activity of ZnTi-layered double hydroxide nanosheets,
1052 *J. Mater. Chem. B.* 1 (2013) 5988. <https://doi.org/10.1039/c3tb21059f>.

1053 [125] M. Li, Z.P. Xu, Y. Sultanbawa, W. Chen, J. Liu, G. Qian, Potent and durable antibacterial
1054 activity of ZnO-dotted nanohybrids hydrothermally derived from ZnAl-layered double

1055 hydroxides, *Colloids Surf. B Biointerfaces*. 181 (2019) 585–592.
1056 <https://doi.org/10.1016/j.colsurfb.2019.06.013>.
1057 [126] Y. Zhang, M. Dai, Z. Yuan, Methods for the detection of reactive oxygen species, *Anal.*
1058 *Methods*. 10 (2018) 4625–4638. <https://doi.org/10.1039/C8AY01339J>.
1059 [127] R.K. Dutta, B.P. Nenavathu, M.K. Gangishetty, A.V.R. Reddy, Studies on antibacterial
1060 activity of ZnO nanoparticles by ROS induced lipid peroxidation, *Colloids Surf. B*
1061 *Biointerfaces*. 94 (2012) 143–150. <https://doi.org/10.1016/j.colsurfb.2012.01.046>.
1062